약학박사학위논문

단백질합성 시작 단계에서 Methionyl-tRNA Synthetase와 AIMP3/p18의 기능적 의의

Functional Significance of Methionyl-tRNA Synthetase and AIMP3/p18 in Translational Initiation

2012년 8월

서울대학교 대학원
약학과 의약생명과학전공
강 태 희

INTRODUCTION

Aminoacyl-tRNA Synthetases (ARSs) are essential enzymes for protein synthesis which catalyze the attachment of amino acid to their cognate tRNA. In higher eukaryote, nine ARSs is forming multisynthetase complex (MSC) with three non-enzymatic cofactors, called ARS-interacting multifunctional proteins (AIMPs). The several functions of ARSs and AIMPs were reported, including signal transduction, immune response, metabolism and cancer related activities. In MSC, methionyl-tRNA sythetase (MRS) ligates methionine to initiator tRNA for translation initiation, and makes a strong interaction with AIMP3, known to be tumor suppressor. Recently, the importance of MRS in global translational regulation was suggested. Although MRS and AIMP3 have many noncanonical functions, it is unclear that why their specific interaction is needed and how the interaction is affected in translational regulation. In translational regulation, the correlation of ARSs and AIMPs is not well-known. In this study, I elucidated the role of MRS and AIMP3 in global translation.

In part 1, dual roles of human MRS was described in the regulation of cytosolic translation and molecular interaction with AIMP3, coupling control of protein synthesis to UV stress. MRS and AIMP3 bound each other via GST homology domain. However MRS was dissociated with AIMP3 under UV

irradiation. The dissociation of AIMP3 and MRS depended on General control nonrepressed 2 (GCN2). MRS was phosphorylated by UV-induced GCN2. The phosphorylation of MRS at Ser662 residue induced a conformational change that is propagated to the N-terminal extension, and then led to AIMP3 releasing from MSC. The modification of MRS affected in the binding ability of initiator tRNA. Therefore, global translation was reduced by phosphorylation of MRS. In addition, MRS cooperated with eukaryotic initiation factor 2 alpha subunit (eIF2α) which responses to DNA damage condition such as UV irradiation. As a result, MRS regulated global translation and tumor suppressor activity of AIMP3 from DNA damage by mechanism which was explained in this study.

In part 2, I demonstrated that AIMP3 regulates translation initiation by mediating transfer of charged initiator tRNA to initiation complex. In MSC, AIMP3 associated with MRS and charged initiator tRNA (Met-$tRNA_i^{Met}$). AIMP3 specifically interacted with Met-$tRNA_i^{Met}$ but not unacylated through the recognition of methionine and acceptor stem. AIMP3 and MRS interacted with eukaryotic initiation factor 2 gamma subunit (eIF2γ). Furthermore, AIMP3 mediated association of MRS and active eIF2γ. Downregulation of AIMP3 reduced ternary complex formation and protein synthesis. As a result, AIMP3 regulated formation of initiation ternary complex, so AIMP3 may regulate the accuracy and efficiency of translation.

Through parts I and II, I elucidated role of MRS and AIMP3 as a regulator of translation initiation. MRS phosphorylation was related with DNA damage response and translational inhibition under UV stress. AIMP3 was dissociated from MRS under UV irradiation, thereby inhibiting ternary complex formation; this chain of events led to reduced rate of protein synthesis. This crosstalk may be important to keep the accuracy and efficiency of protein synthesis.

Keywords : Methionyl-tRNA synthetase (MRS), General control nonrepressed 2 (GCN2), eukaryotic initiation factor 2 (eIF2), initiator tRNA, ARS-interacting multifunctional protein 3 (AIMP3), Translation

Student ID : 2006-30453

ABBREVIATIONS

ARS : Aminoacyl-tRNA synthetase

MSC : Multisynthetase complex

AIMP : ARS-interacting multifunctional protein

MRS : Methionyl-tRNA synthetase

GCN2 : General control nonrepressed 2

eIF : Eukaryotic initiation factor

$tRNA_i^{Met}$: initiator tRNA

$Met\text{-}tRNAi^{Met}$: Charged initiator tRNA

MBP : Maltose binding protein

WCL : Whole cell lysate

EPRS : Glutamyl-prolyl-tRNA synthetase

p-eIF2α : phosphorylated eIF2α

BiFC : Bimolecular fluorescence complement

VN : Venus N-terminus

VC : Venus C-terminus

IP : Immunoprecipitation

Si-RNA : Small interference RNA

MEF : Mouse embryonic fibroblast

AP : Alkaline phosphatase

CBB : Coomassie brilliant blue

KD : Kinase domain

$tRNA_e^{Met}$: Elonagator tRNA

EV : Empty vector

p-MRS : Phosphorylated MRS

WT : Wild type

CD : Circular dichroism

PL : Peptide linker

GAIT : gamma interferon inhibitor of translation

KRS : Lysyl-tRNA synthetase

HRS : Histidyl-tRNA synthetase

IF : Immunofluorescence

SF : Serum free

RT : Room temperature

TCA : Trichloroacetic acid

ERS : Glutamyl-tRNA synthetase

RRS : Arginyl-tRNA synthetase

eEF1ε1 : Eukaryotic elongation factor 1 epsilon 1

acK : Acetylate lysine

DMEM : Dulbecco’s modified Eagle’s medium

dFx : Dinitro-flexizyme

CHX : Cycloheximide

CONTENTS

LIST OF FIGURES

(Part I.)

(Part II.)

PART I.

Dual Role of Methionyl-tRNA Synthetase in the Translational Regulation and Translocation of Tumor Suppressor Activity AIMP3/p18

Keywords : MRS, AIMP3, Translation, GCN2, initiator tRNA, eIF2α

ABSTRACT

Mammalian methionyl-tRNA synthetase (MRS) plays an essential role in the initiation step of translation by transferring methionine to initiator tRNA ($tRNA_i^{Met}$) and also provides a cytosolic anchoring site for AIMP3/p18, a potent tumor suppressor that is translocated to the nucleus for DNA repair upon DNA damage. However, the regulation of these two seemingly unrelated functions by the enzyme is unknown. Here, I identified that AIMP3 is released from MRS by UV-induced stress. Dissociation was induced by phosphorylation of MRS at Ser662 by general control nonrepressed-2 (GCN2) following UV irradiation. Substitution of Ser662 to Asp (S662D), which mimics GCN2-mediated phosphorylation, induced a conformational change in MRS and significantly reduced its interaction with AIMP3. The S662D mutant also exhibited significantly reduced MRS catalytic activity due to the loss of $tRNA^{Met}$ binding, resulting in downregulation of global translation. Inactivation of GCN2-induced phosphorylation either at eIF2 subunit α (eIF2α) or MRS augmented the role of the counterpart, suggesting that MRS would provide the complementary gateway for eIF2α upon DNA damage. This work is the first report on the regulation of global translation mediated by aminoacyl-tRNA synthetase, especially MRS, which herein identified as a new GCN2 substrate. In addition,

this research suggests a dual role of MRS: (1) MRS acts as a co-regulator with eIF2α for GCN2-mediated translational inhibition. (2) MRS couples translational inhibition and DNA repair following DNA damage via release of bound tumor suppressor AIMP3 for the nuclear translocation.

INTRODUCTION

Translational regulation is a mechanism by which genetic expression can be modulated to deal with various biological conditions. Deregulation or dysregulation of protein synthesis is frequently observed in diseases, especially in cancer; therefore, accurate translational control should be assured for the maintenance of normal growth and proliferation (1,2). Under stress conditions, global translational control mainly occurs at the initiation of translation by modification of eukaryotic initiation factors (eIFs). Phosphorylation of eIF2 subunit α (eIF2α) is one of the key regulatory mechanisms because it impairs formation of ternary complex (TC), which comprises eIF2, GTP, and methionine (Met)-charged initiator tRNA (Met-$tRNA_i^{Met}$), blocking further rounds of translation initiation (3).

Aminoacyl-tRNA synthetases (ARSs) are essential components for translation, catalyze the attachment of their corresponding amino acids to its cognate tRNA (4,5). Methionyl-tRNA synthetase (MRS) is distinguished by its participation in translation initiation by charging $tRNA_i^{Met}$ with methionine to produce Met-$tRNA_i^{Met}$, which is indispensable for TC formation. MRS has been also found in the nucleoli, where it may play a role in the biogenesis of ribosomal RNA (6). In addition, MRS may charge methionine to non-cognate

tRNAs under oxidative stress, resulting in reduced translational fidelity (7). Stable overexpression of the MRS substrate $tRNA_i^{Met}$ can drive proliferation and oncogenic transformation (8). These reports indicate the unique significance of MRS in translational control; however, little is known regarding the regulation of its catalytic activity and non-canonical activities.

In higher eukaryote, nine different ARSs including MRS form an intriguing macromolecular complex, the multi-synthetase complex (MSC), with three non-enzymatic cofactors designated AIMP1/p43, AIMP2/p38, and AIMP3/p18 (4,5,9). In this complex, MRS forms a specific association with the tumour suppressor AIMP3 (10-13). While AIMP3 is mainly anchored to MRS in the cytosol, it also activates ATM and ATR in the nucleus upon DNA damage or oncogenic stress (11,14,15). However, it is unclear whether nuclear AIMP3 is actually dissociated from the cytosolic MSC. Translational regulation and the DNA damage response should be closely coupled for the precise control of cell survival. I hypothesized that there should be crosstalk between nuclear translocation of AIMP3 and translational control following DNA damage, which affects both the cell cycle and protein synthesis. This study was designed to address the roles of MRS in the regulation of translation and translocation of the tumour suppressor AIMP3 and its underlying molecular mechanism.

RESULTS

AIMP3 and MRS Interact via GST-like Domains

MRS shows an especially variable structural organization according to species (16). Human MRS contains unique non-catalytic extensions, GST-homology and WHEP domains at the amino (N)- and the carboxy (C)-termini, respectively (17) (Figure I-1A). AIMP3 also contains the GST-homology domain in the C-terminal side. Although interaction between MRS and AIMP3 has been reported previously (10-14), which domains are in charge of the interaction remains unknown. To map the interaction between MRS and AIMP3, MRS deletion fragments, D1 (GST-like domain), D2 (catalytic domain), and D3 (tRNA binding domain), and N- and C-terminal domains of AIMP3 were used for yeast two hybrid assay. In the pairs of LexA-AIMP3 and B42-MRS and its derivatives, AIMP3 strongly interacted with MRS D1 as well as full-length MRS both in the plates of Ura^-, His^-, Trp^-, Leu^-/gluocose (Leu^-) and Ura^-, His^-, Trp^-/galactose containing X-gal and raffinose (X-gal) media (Figure I-1B). The interaction between MRS and AIMP3 as well as C-terminus of AIMP3 was also reflected by growth of yeast colony on the LEU^- media by the pairwise test of LexA-MRS and B42-AIMP3 fragments (Figure I-1C). These results show that MRS and AIMP3 can interact via their D1 and C-terminal domains, respectively. Next, I

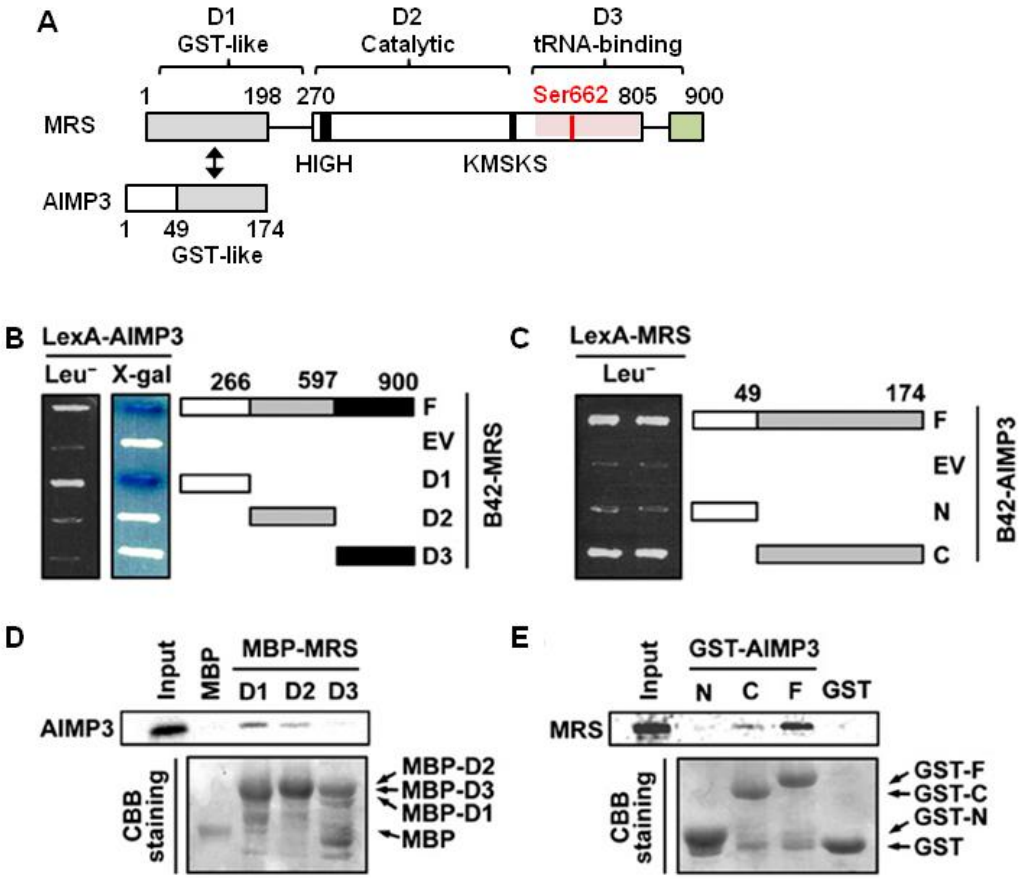

Figure I-1. Schematic representation of MRS and AIMP3 domains and their interaction. (A) Schematic representation of functional domain arrangements in human MRS and AIMP3. Human MRS contains a eukaryote-specific N-terminal extension that has homology to GST (grey). The central catalytic domain (white) contains class I signature motifs such as HIGH and KMSKS. The C-terminal domain (pink for anti-codon binding and green for WHEP domains) interacts with $tRNA^{Met}$. The GST-homology domain of MRS makes a specific interaction with another GST-homology domain (grey) of AIMP3 (see Figure I-1B–1E). Ser662 is phosphorylated by UV-activated GCN2. D1 (1–266 residues), D2 (267–596), and D3(597–900) are the deletion fragments of MRS that were used for the *in vitro* pull-down and kinase assays (see

Figure I-1D, I-1E, and Figure I-4F). **(B)** Different domains of MRS D1, D2, and D3 were expressed as B42-fusion proteins in yeast and their ability to bind AIMP3 fused to LexA was determined. Positive interactions were identified by cell growth on LEU^- (left) and blue colony formation on X-gal (right) media. **(C)** AIMP3 domains (N: residues 1–49 and C: residues 50–174) were expressed as B42-fusion proteins and their ability to interact with LexA-MRS was determined. Positive interactions were identified by cell growth on LEU^- medium. **(D)** Radioactively labeled AIMP3 was incubated with different domains of MBP-MRS immobilized with amylose resin. Co-precipitated AIMP3 was detected by autoradiography. **(E)** Radioactively labeled MRS was incubated with the F- (full), N-, and C-domains of AIMP3 precipitated with glutathione-sepharose. Co-precipitation of MRS was detected by autoradiography.

conducted pull down assays to conform the interaction of MRS and AIMP3. When AIMP3 was incubated with maltose binding protein (MBP)-fused MRS domains, AIMP3 showed strong interaction with MBP-MRS D1 although it also slightly interacted with MBP-MRS D2 (Figure I-1D). Binding of MRS to AIMP3 domains was determined by co-precipitation of MRS with GST-AIMP3 domains and the result showed interaction of MRS with C-terminal domain of AIMP3 (Figure I-1E). Taken together, all these results demonstrated that MRS and AIMP3 interact via their GST-homology domains (Figure I-1A).

AIMP3 Is Released from MRS and Translocated to Nucleus upon DNA Damage

AIMP3 was known to be located in nucleus following UV-irradiation (11). Therefore, I investigated whether UV-induced DNA damage affects the interaction between MRS and AIMP3 in the cytosol. HeLa cells were UV-irradiated and harvested at the indicated times and whole cell lysate (WCL) was immunoprecipitated with MRS antibody to determine the level of bound proteins by immunoblotting. While interaction between MRS and AIMP3 was maintained without UV irradiation, AIMP3 bound to MRS was gradually decreased after UV irradiation (Figure I-2A). Binding of EPRS (glutamyl-prolyl-tRNA synthetase), another component of MSC, to MRS was unaffected by UV

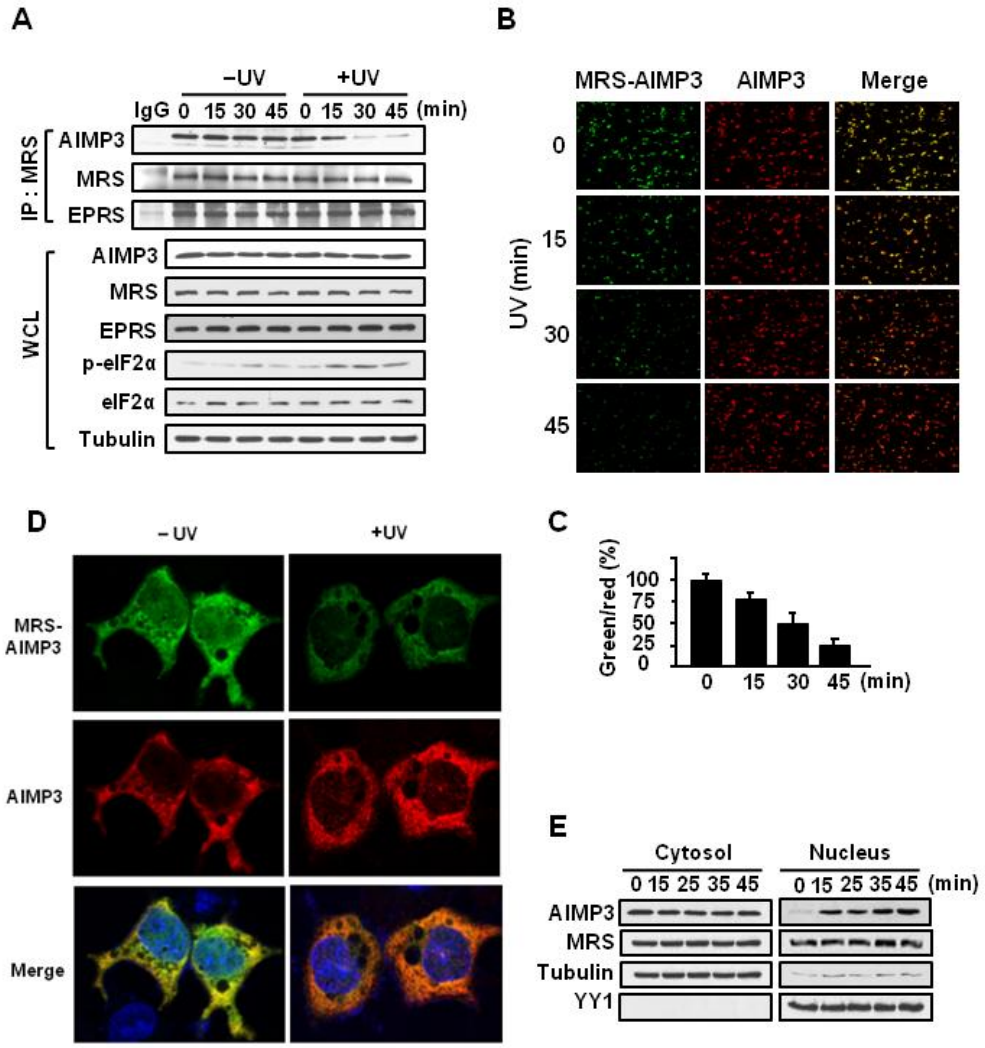

Figure I-2. AIMP3 dissociates from MRS and translocates into nucleus following UV irradiation. (A) Interaction of AIMP3 and EPRS with MRS in UV-irradiated HeLa cells (60 J/m^2) was determined by immunoprecipitation (IP). Cells were lysed and immunoprecipitated with anti-MRS antibody. Coimmunoprecipitated proteins were separated by SDS-PAGE and detected with each specific antibody. Levels of AIMP3, MRS, EPRS, and phosphorylation of eIF2α in whole cell lysates (WCL) were also detected by immunoblotting. **(B)** The dissociation between AIMP3 and MRS was determined by biomolecular fluorescence complementation assay (BiFC). HCT116 cells

co-transfected with Flag-AIMP3-VN (N-terminal nonfluorescent fragments of Venus) and HA-MRS-VC (C-terminal nonfluorescent fragments of Venus) were irradiated by UV. Reconstitution of Venus fluorescence by close proximity of VN and VC resulting from the interaction of MRS and AIMP3 is shown by green fluorescence. AIMP3 alone was observed by red fluorescence using Alexa Fluor 555-conjugated anti-Flag antibody. **(C)** The graph presents the relative ratios of the green (MRS:AIMP3 complex) versus red (AIMP3) spot counts (lower panel). Data are represented as mean +/− SD (n = 3). **(D)** In the same BiFC system using HeLa cells, the dissociation of AIMP3 from MRS and nuclear localization was monitored at higher magnification. The red fluorescence from AIMP3 merged with PI-stained nucleus forming foci. **(E)** Nuclear translocation of AIMP3 was analyzed by immunoblotting after cell fractionation. YY1 and tubulin were used as nuclear and cytosolic markers, respectively.

irradiation, implying that AIMP3 was specifically released from MSC (Figure I-2A). The dissociation of MRS and AIMP3 was coincident with induction of phosphorylated eIF2α (p-eIF2α), a known marker for UV-dependent translational inhibition (18). To visualize the direct interaction between MRS and AIMP3, I used bimolecular fluorescence complement (BiFC) analysis by fusing Venus N-terminal (VN) and C-terminal (VC) fragments to AIMP3 and MRS, respectively (19). VN and VC are non-fluorescent fragments; therefore, single transfection of Flag-AIMP3-VN or HA-MRS-VC did not emit fluorescence by themselves (Figure I-3A). VN and VC did not reconstitute Venus fluorescence by self-association even when both fragments were expressed together. Only co-transfection of the two fusion proteins, Flag-AIMP3-VN and HA-MRS-VC, produced green fluorescence, indicating that the green fluorescence resulted from the association of MRS and AIMP3 (Figure I-3A). When HCT116 cells were transfected with the two fusion proteins, the number of the green fluorescence cells decreased after UV irradiation, supporting UV-induced dissociation of MRS and AIMP3 (Figure I-2B left column). Cellular levels of AIMP3 monitored by red fluorescence were not affected by UV irradiation, indicating that UV stress did not affect AIMP3 level or cell viability (Figure I-2B middle column). Count of green versus red fluorescences indicates the gradual dissociation of MRS and AIMP3 (Figure I-2C). When BiFC fluorescence was

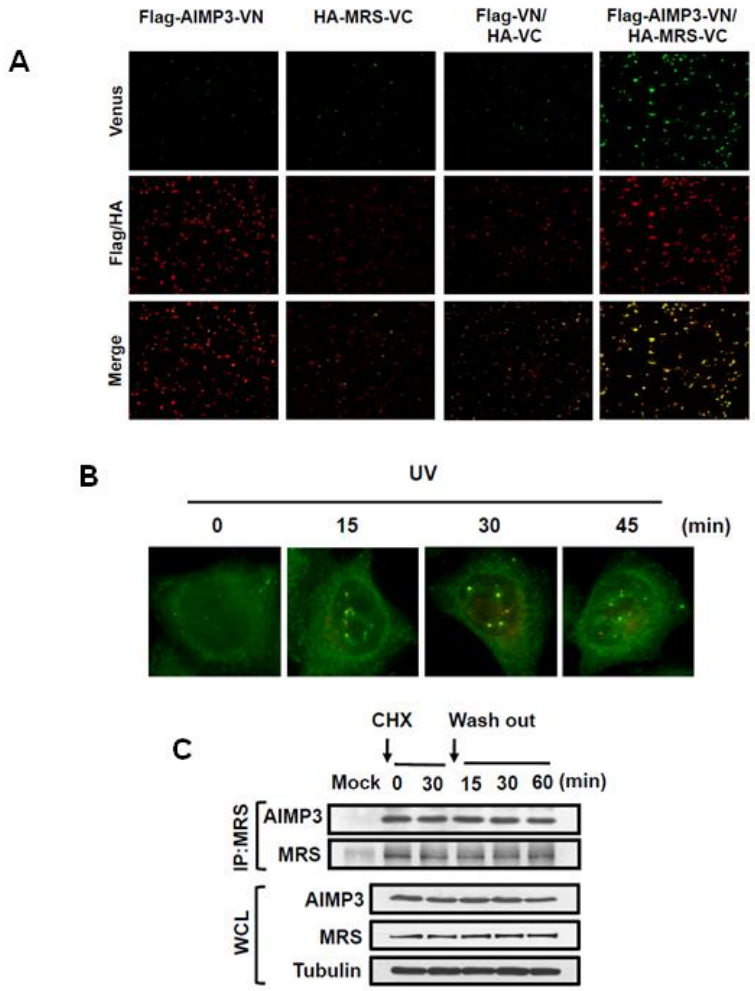

Figure I-3. AIMP3 dissociates from MRS and translocates to the nucleus following UV irradiation but not by cycloheximide treatment. (A) AIMP3 and MRS were cloned into pBiFC-VN173 and pBiFC-VC155, respectively, resulting expression of Flag-AIMP3-VN (nonfluorescent N-terminal fragment of Venus) and HA–MRSVC (nonfluorescent C-terminal fragment of Venus) fusion proteins. HCT116 cells were transfected with single or both of fusion proteins and reconstitution of Venus fluorescence by close proximity of VN and VC was observed by fluorescence microscopy (200x). Control vectors, pBiFC-VN173 and pBiFC-VC155, were also

tranfected into HCT116 cells together as a negative control. Venus fluorescence was observed only in the cells cotransfected with Flag-AIMP3-VN and HA-MRS-VC (green color). Autofluorescence from Flag-VN and HA-VC, Flag-AIMP3-VN, or HA-MRS-VC was weak and could be differentiated from reconstituted green fluorescence. Flag or HA (only for single transfection of HA–MRS-VC) was observed by red fluorescence using Alexa Fluor 555-conjugated anti-Flag or HA Antibody for transfection control. **(B)** HeLa cells transfected with GFP-AIMP3 were irradiated by UV and cells were fixed and stained with propidium iodide. Cellular localization of GFP-AIMP3 was monitored by fluorescence microscopy (600x). **(C)** HeLa cells were treated with cycloheximide (CHX) for 30 min. After washing, the cells were harvested at the indicated times. Lysates were immunoprecipitated with anti-MRS antibody for determined of AIMP3 dissociation. Bound proteins and WCL were detected by immunoblotting. Dissociation of AIMP3 and MRS was not observed by CHX treatment.

monitored at higher magnification, the intensity of green fluorescence in each cell was decreased by UV irradiation (Figure I-2D). In addition, UV-dependent nuclear foci formation of AIMP3 was observed demonstrating that dissociation of AIMP3 from MRS is accompanied by its nuclear localization. UV-induced nuclear foci formation was also observed by overexpression of GFP-AIMP3 in HeLa cells (Figure I-3B). UV-induced nuclear translocation of AIMP3 was reconfirmed by cell fractionation and immunoblotting experiments (Figure I-2E). Although decrease of AIMP3 in the cytosol was not apparent, increase of AIMP3 in the nucleus following UV irradiation was clearly demonstrated. A portion of MRS was also found in the nuclear fraction as previously reported (6), however this localization was regardless of UV irradiation. Dissociation of MRS and AIMP3 was not observed when *de novo* protein synthesis was blocked by cycloheximide treatment (Figure I-3C), suggesting that dissociation of MRS and AIMP3 is specific to UV-induced stress.

Phosphorylation of MRS by UV-activated GCN2 Is Responsible for Dissociation of AIMP3

Since UV irradiation induced dissociation of MRS and AIMP3, I hypothesized that GCN2 may be involved since it is known to induce UV-dependent translation block via phosphorylation of eIF2α (18, 20-22). To test this

possibility, I used specific small interference RNA (si-RNA) to knock down GCN2 in HeLa cells. MRS and AIMP3 disassociated following UV irradiation in cells transfected with control si-RNA; however, MRS and AIMP3 did not disassociate with knockdown of GCN2 (Figure I-4A). Similar experiments were conducted using $GCN2^{+/+}$ and $GCN2^{-/-}$ mouse embryonic fibroblast (MEF) cells. MRS and AIMP3 did not disassociate following UV irradiation in $GCN2^{-/-}$ cells, in contrast to the wild-type cells (Figure I-4B). Total protein level of AIMP3 and MRS was basally reduced in $GCN2^{-/-}$ MEF cells compared to $GCN2^{+/+}$ MEF, suggesting a close relationship among GCN2, MRS and AIMP3. These data suggest that GCN2 is involved in controlling interaction between MRS and AIMP3.

To investigate post-translational modifications of MRS and/or AIMP3 following UV irradiation, two-dimensional polyacrylamide gel electrophoresis (2D-PAGE) was used to compare the electrophoresis pattern of the two proteins with and without irradiation. UV irradiation generated additional spots of MRS that were shifted to the acidic side, which disappeared by the treatment of alkaline phosphatase (Figure I-4C). In contrast, no obvious UV-induced acidic protein shifts were observed for AIMP3. Based on these results, I suspected that MRS may be phosphorylated by GCN2. To confirm this possibility, MRS

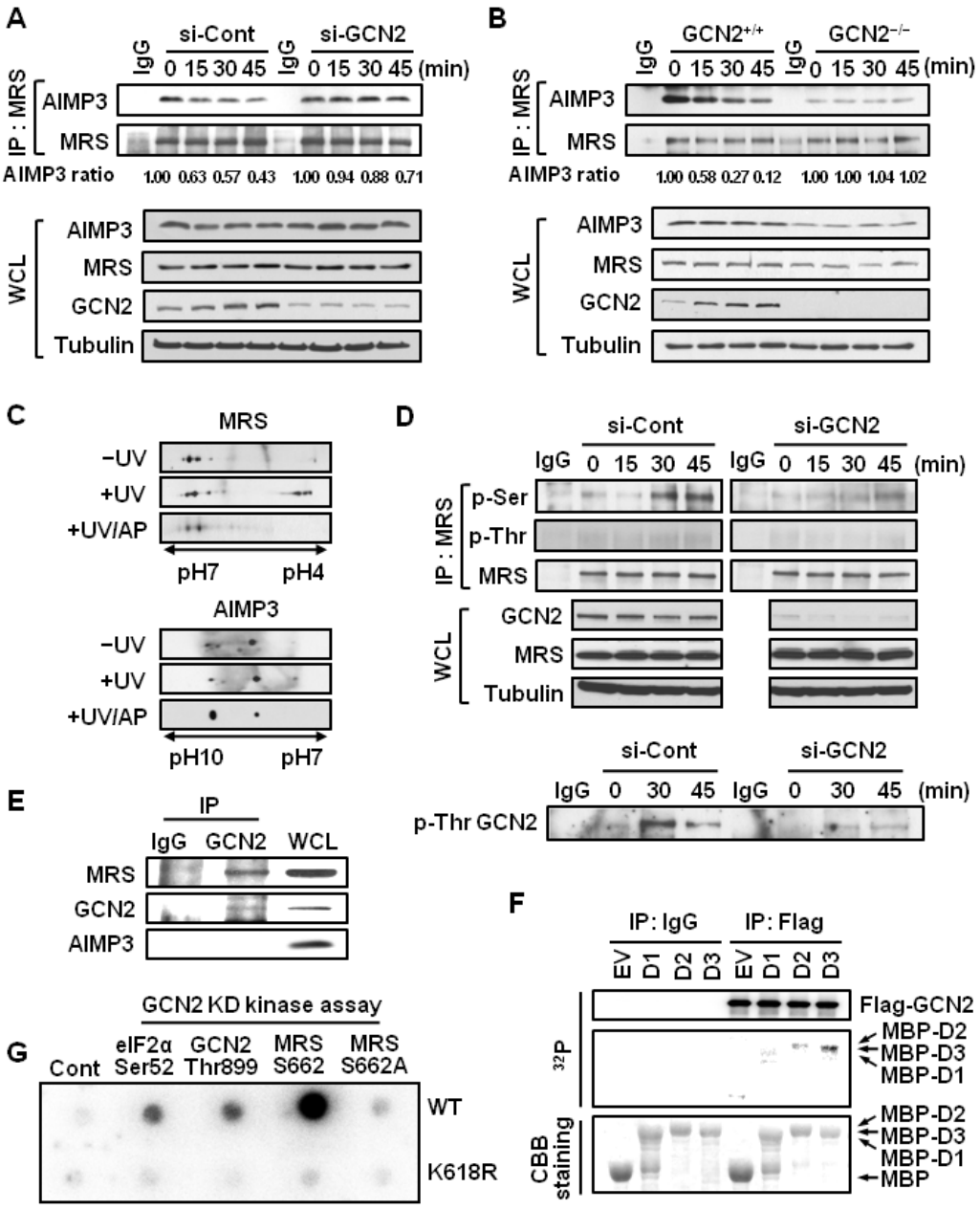

Figure I-4. GCN2-induced phosphorylation is responsible for the dissociation of MRS and AIMP3 by UV irradiation. (A and B) HeLa cells transfected with si-control or si-GCN2 for 72 h **(A)** or $GCN2^{+/+}$ and $GCN2^{-/-}$ MEFs **(B)** were irradiated by UV.

Interaction between MRS and AIMP3 was detected by IP and immunoblotting. **(C)** After UV irradiation in HeLa, cell were incubated in serum free media during 30min and lysed. Proteins (500 μg) from HeLa cells were separated by 2D-PAGE. Half of the UV-irradiated samples were treated with alkaline phosphatase (AP) for dephosphorylation. **(D)** The effect of GCN2 knockdown on MRS phosphorylation was detected using anti-p-Serine or anti-p-Threonine antibodies (upper). UV-dependent phosphorylation of GCN2 at Thr899 was validated using p-Threonine antibody. **(E)** Cellular interaction of GCN2 with MRS was observed in UV-irradiated HeLa cells. **(F)** Lysates from flag-GCN2 transfected 293 cells were immunoprecipitated with mock IgG and flag antibody. Immunoprecipitated Flag-GCN2 was incubated with [γ-^{32}P]ATP and MBP-tagged domains of MRS, D1, D2, and D3 (Figure 1A). Reaction samples were separated by SDS-PAGE, stained with Coomassie brilliant blue (CBB), and dried for detection of radioactive protein. The phosphorylation of protein was determined by autoradiography. **(G)** The immobilized GST-GCN2 kinase domain (KD) was mixed with biotinylated synthetic peptides containing known sequences of GCN2 substrates and [γ-^{32}P]ATP. The MRS peptide containing Ser662, but not S662A, was radioactively labeled, similar to the positive control peptides GCN2 Thr899 and eIF2α Ser52 (Ser51 in mouse). Kinase reaction done without any peptide was used as control.

was immunoprecipitated after UV irradiation and immunoblotted with phospho-specific antibodies in control and GCN2-knockdown cells. Phosphorylation of MRS at serine residues was observed in MRS extracted from the control cells, which was significantly reduced in GCN2-knockdown cells (Figure I-4D upper panel) Under the same conditions, UV-dependent activation of GCN2 was confirmed by immunoblotting using p-Thr 898 antibody specific to GCN2 (Thr899 residue in human) as previously reported (23) (Figure I-4D lower panel). Importantly, MRS, but not AIMP3, was co-immunoprecipitated with GCN2 (Figure I-4E) following UV irradiation, suggesting MRS is a direct substrate of GCN2.

I introduced both initiator and elongator $tRNA^{Met}$ ($tRNA_e^{Met}$) into HeLa cells and determined their effect on the interaction between MRS and AIMP3, since GCN2 is known to be activated by uncharged tRNA (24). I confirmed the enhanced expression of the transfected tRNAs by northern blot analysis with their specific probes (Figure I-5A). Increased expression of both tRNAs triggered dissociation of AIMP3 from MRS and phosphorylation of MRS (Figure I-5B). Introduction of these tRNAs enhanced p-GCN2 and p-eIF2α as previously reported (25). Deprivation of amino acids also activates GCN2 by increasing free tRNAs (18) and I also observed separation of AIMP3 from MRS and simultaneous p-eIF2α induction by methionine deprivation for 1 hr,

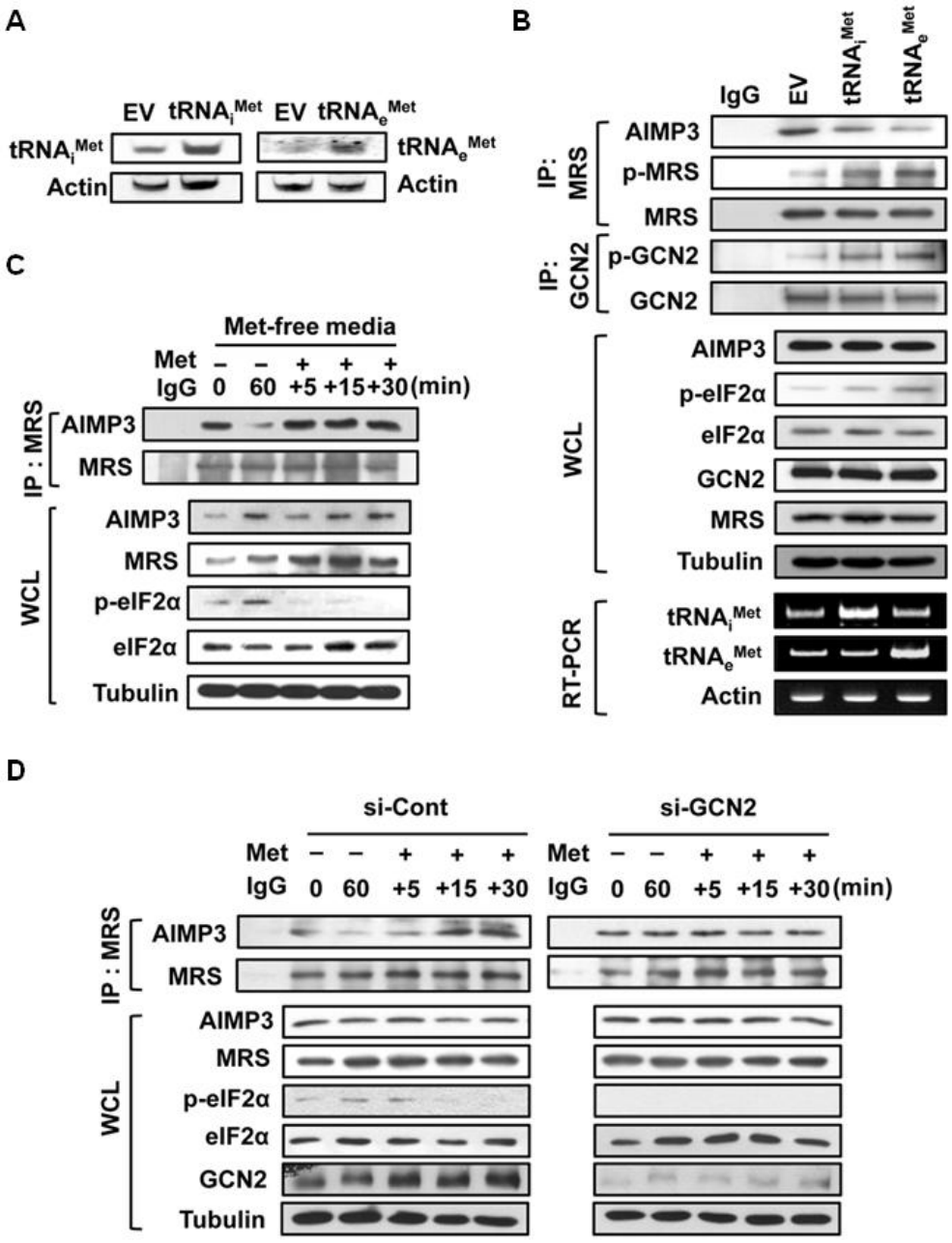

Figure I-5. MRS phosphorylation and AIMP3 dissociation were mediated by GCN2. (A) HeLa cells were transfected with pGEM-T-Easy vector encoding initiator and elongator tRNA^{Met}. After 24 h, total RNA was purified, and tRNA expression levels

were analyzed by Northern blotting using a biotinylated probe to confirm increased expression of transfected initiator and elongator $tRNA^{Met}$. Actin was used as a loading control. **(B)** HeLa cells transfected with pGEM-T-Easy vector encoding initiator and elongator $tRNA^{Met}$ were lysed after 24-h incubation. Empty vector (EV)-transfected cells were used as a control. MRS and GCN2 were immunoprecipitated. Co-IP AIMP3 and phosphorylated MRS (p-MRS) and p-GCN2 were determined by specific antibodies. Expression of each tRNA was assayed by RT-PCR. **(C)** HeLa cells were incubated in methionine-free media for 1 h and then methionine was added in the media. Cells were harvested and the association between MRS and AIMP3 was monitored by immunoblotting. **(D)** Methionine-dependent interaction between AIMP3 and MRS was monitored as described in C, using HeLa cells transfected with si-Control (Cont) or si-GCN2 for confirmation of GCN2 dependency.

which was recovered within 5 min by methionine addition (Figure I-5C). As expected, this methionine-sensitive separation was abolished when GCN2 was knocked (Figure I-5D). Taken together, these results suggest that GCN2 is responsible for phosphorylation of MRS resulting disassociation of AIMP3 from MRS.

To identify the phosphorylation site(s) on MRS, two different MRS proteins were prepared. First, endogenous MRS was immunoprecipitated from UV-treated HeLa cells. Second, MRS was expressed as a MBP-fusion protein and subjected to an *in vitro* GCN2 kinase assay. MRS bands were extracted from gels after SDS-PAGE and proteins were digested and processed for nano LC-MS/MS analysis. Based on the Mascot search results, phosphorylation at Ser229, Ser472, and Ser662 was detected in both cases (Figure I-6A). I conducted the GCN2 kinase assay in the presence of [γ-^{32}P]ATP using MBP-fused MRS domains (D1, D2, and D3, and Figure 1A). A relatively strong radioactivity was detected in the D3 domain harboring Ser662 (Figure I-4F), and the signal was not observed by incubation with inactive form of GCN2 (Figure I-6B).

To further validate this site, the biotinylated MRS peptide spanning Ser662 and the same peptide with S662A substitution was synthesized. Although GCN2-induced phosphorylation was apparent in the wild-type (WT) MRS peptide, it was not observed in S662A peptide (Figure I-4G). The two

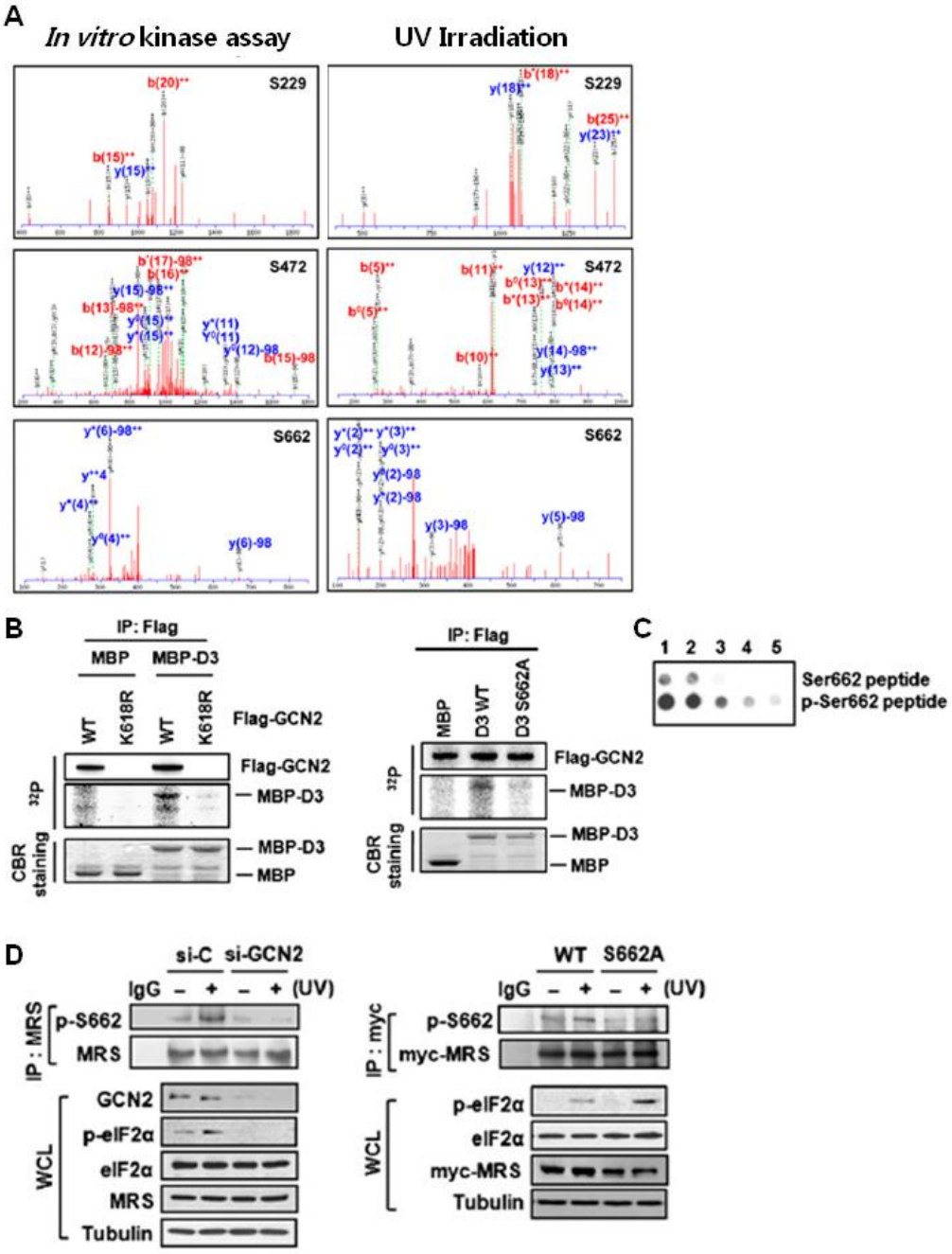

Figure I-6. Determination of GCN2-induced phosphorylation sites of MRS. (A) MRS proteins, which were phosphorylated by *in vitro* kinase reaction and

immunoprecipitated from UV-treated HeLa cells, were processed for nano LC-MS/MS analysis as described in Materials and Methods. Phosphorylation at S229, S472, and S662 was detected in both cases. Detected peptide sequences spanning the phosphorylation site and the peaks for the equivalent fragment ions are shown ($P < 0.05$). **(B)** MBP-MRS D3 WT was incubated with GCN2 WT or the GCN2 K618R inactive mutant immunoprecipitated from 293T cells (Left) and MRS D3 WT and the S662A mutant were subjected to GCN2 kinase assay for *in vitro* kinase assay (Right). Phosphorylation signal was detected by autoradiography. **(C)** Specificity of p-Ser662–specific antibody to peptide harboring p-Ser662 was analyzed. MRS peptides (GMFVSKFFGGYVPEC) with or without phosphoserine residue were serially diluted, spotted onto PVDF membrane, and then immunoblotted using p-Ser662–specific antibody. Concentrations of peptides used were 5 μM (lane 1), 2.5 μM (lane 2), 1.25 μM (lane 3), 0.625 μM (lane 4), and 0.313 μM (lane 5). **(D)** MRS was immunoprecipitated from HeLa cells transfected with si-control (si-C) or si-GCN2 and p-MRS was detected using p-Ser662–specific antibody (Left). Exogenous MRS was immunoprecipitated from stable HeLa cells expressing MRS WT or S662A mutant and subjected to immunoblotting using p-Ser662–specific antibody (Right).

positive control peptides derived from GCN2 and eIF2α (22, 23, 26) and a negative control, the GCN2 K618R inactive mutant, validated the GCN2 kinase assay. I next detected MRS phosphorylation using p-Ser662–specific antibody and found that UV-dependent p-Ser662 signal was specific to GCN2 and Ser662 residue (Figure I-6C and D). This result suggests that under conditions of UV stress, GCN2 mediates phosphorylation of MRS at Ser662.

Phosphorylation of MRS at Ser662 residue induces a conformational change to release AIMP3

To determine the effect of GCN2-induced phosphorylation on the interaction between MRS and AIMP3, I introduced S229D, S472D, and S662D mutations into MRS, and examined how these phosphorylation-mimicking mutations would affect the interaction of MRS with AIMP3. Each of the three GST-MRS mutants precipitated with glutathione-Sepharose beads was incubated with radioactively labeled AIMP3 and the binding of AIMP3 was determined by autoradiography. The binding of the MRS S662D mutant to AIMP3 was decreased compared to WT and the other mutants (Figure I-7A). When His-AIMP3 was purified from co-expression system of S-MRS and His-AIMP3 using Nickel-affinity column, S-MRS WT, but not the S-S662D mutant, was co-purified with AIMP3 as well (Figure I-7B). I next established HeLa cell lines

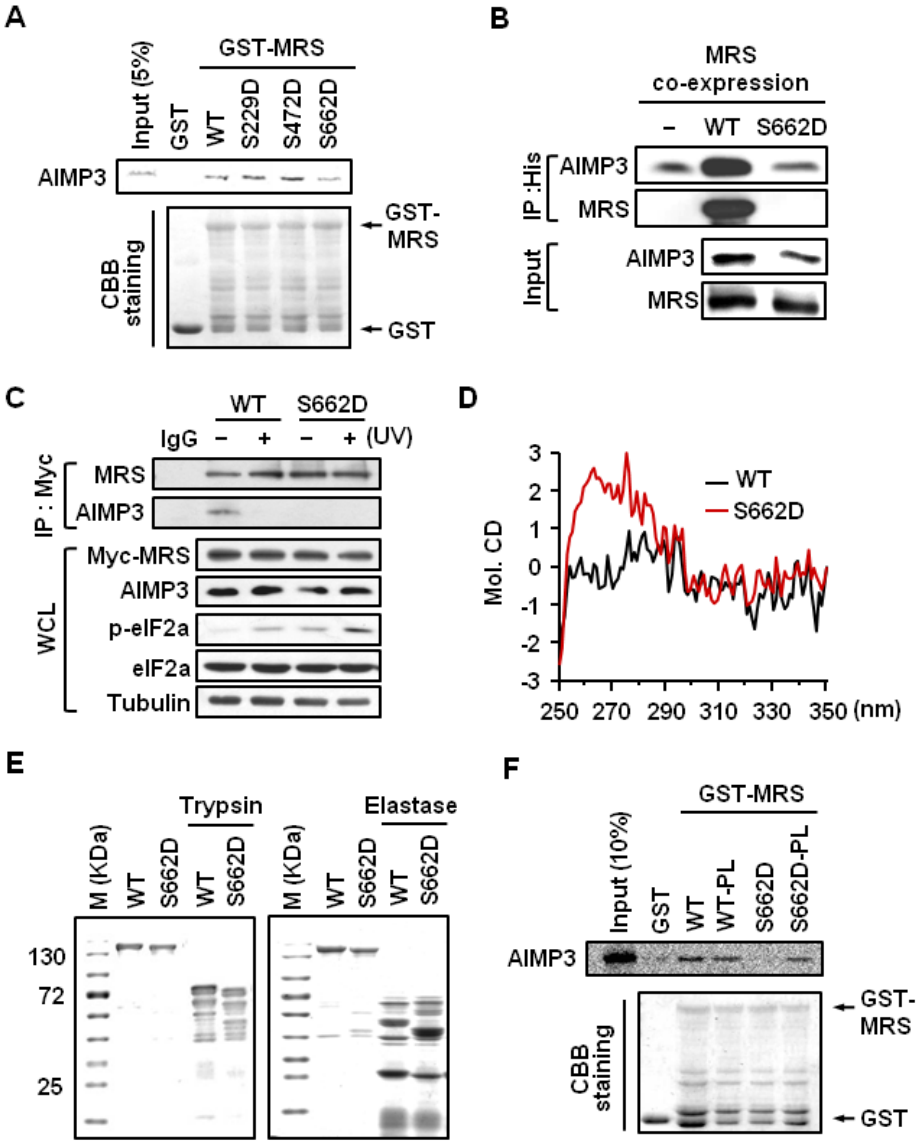

Figure I-7. GCN2-induced phosphorylation may trigger a conformational change in MRS and induce AIMP3 dissociation. (A) [^{35}S]Methionine-labeled AIMP3 was synthesized by *in vitro* transcription and translation coupled kit and incubated with immobilized GST-MRS WT and MRS mutants (S229D, S472D, and S662D). Radioactivity from bound AIMP3 was detected by autoradiography. **(B)** S-tagged MRS WT or the S662D mutant was co-expressed with His-tagged AIMP3 using dual protein

expression system and AIMP3 was purified by Ni-NTA agarose affinity chromatography. Copurification of AIMP3 and MRS was determined by immunoblotting. **(C)** The interaction of MRS WT and the S662D mutant with AIMP3 was determined by IP using HeLa cells stably expressing Myc-tagged MRS WT and S662D mutant. Cells were lysed and immunoprecipitated with anti-myc antibody. Coimmunoprecipitated proteins were separated by SDS-PAGE and detected with each specific antibody. **(D)** CD spectra of the purified MBP-MRS WT and S662D proteins were obtained using a Jasco J-815 CD spectrometer at 25℃ in the near UV range of 250–350 nm. **(E)** Purified MBP-MRS proteins were digested with trypsin or elastase, and the cleaved fragments were visualized by CBB staining. **(F)** For effect of MRS conformational change in dissociation of AIMP3, PL (GGGGS) was inserted between residues 233 and 234 of MRS WT and the S662D mutant to provide conformational flexibility. The native and PL-inserted MRS proteins (WT and the S662D mutant) were subjected to an *in vitro* pull-down assay with radioactively labeled AIMP3. Radioactive AIMP3 was detected by autoradiography.

stably expressing MRS WT or S662D mutant by G418 selection. When these exogenous MRS were immunoprecipitated using anti-Myc antibody, AIMP3 was not co-precipitated with the MRS S662D mutant in contrast to MRS WT (Figure I-7C). MRS S662A mutant interacted stably with AIMP3 regardless of UV stress (Figure I-8A). These results suggest that phosphorylation of MRS at Ser662 may decrease the binding affinity of MRS to AIMP3.

Since Ser662 is distantly located from the N-terminal extension of MRS that is involved in the interaction with AIMP3 (Figure I-1A), phosphorylation at Ser662 may not directly affect the interaction of MRS with AIMP3. Instead, phosphorylation at Ser662 may induce a conformational change that leads to dissociation of AIMP3. This hypothesis was tested by comparing circular dichroism (CD) spectra of MRS WT and the S662D mutant. The MRS S662D mutant had different CD spectrum in the near UV range between 250 and 350 nm (Figure I-7D), suggesting a difference in its tertiary structure. The two proteins were also subjected to trypsin and elastase digestion to compare the difference in accessibility to these proteases. With both enzymes, the MRS S662D mutant showed a slightly different digestion pattern (Figure I-7E), further suggesting a conformational difference. Next, I inserted a Gly-Gly-Gly-Gly-Ser peptide linker (PL) into the region between the N-terminal AIMP3 binding and catalytic domains of MRS WT and of the S662D mutant. The insertion of

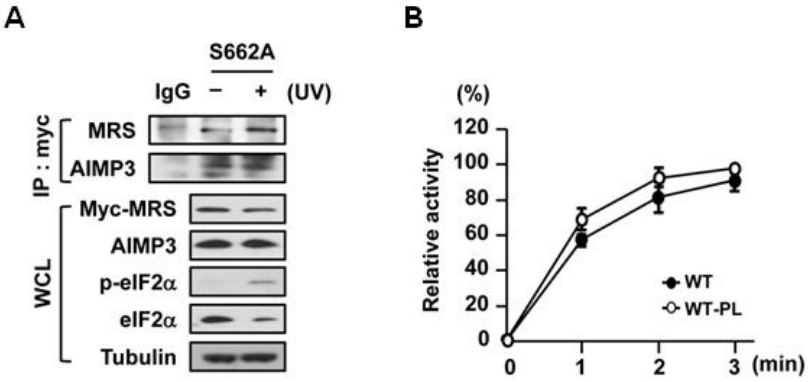

Figure I-8. Effects of alanine substitution or peptide linker insertion on MRS function. (A) The MRS S662A mutant was immunoprecipitated from stable HeLa cells and the bound AIMP3 upon UV was detected by immunoblotting. WCL, whole-cell lysates. **(B)** The aminoacylation assay was performed with purified His-MRS with or without peptide linker insertion. The activities at 3min of MRS WT were normalized to 100%. Results are presented as mean as mean ± SD (n = 3).

this flexible peptide is expected to loosen the conformational linkage between the AIMP3-binding N-terminal region and the Ser662-harboring C-terminal domain and provide conformational flexibility. However, the selected position for the PL insertion was not expected to alter MRS activity nor protein-protein interaction (13, 27). Indeed, in the wild-type background, the aminocylation activity of MRS was not influenced by PL-insertion (Figure I-8B), and AIMP3 also bound to the normal and PL-inserted MRS with similar affinity (Figure I-4F left lanes). In contrast, the insertion of the PL into MRS S662D restored its ability to bind AIMP3 (Figure I-4F right lanes). These data suggest that Ser662 phosphorylation may induce a conformational change that is propagated to the N-terminal extension, releasing the bound AIMP3.

Phosphorylation of MRS at Ser662 residue reduced catalytic activity and global translation

Ser662 is located within the anticodon-binding motif (28, 29), therefore, its mutation may disrupt tRNA binding and aminoacylation activity. This hypothesis was tested by *in vitro* tRNA binding and aminoacylation assays. $tRNA_i^{Met}$ was radioactively synthesized by *in vitro* transcription in the presence of [α-^{32}P]UTP and reacted with MRS WT and the S662D mutant. When the reaction mixtures were separated by native PAGE and autoradiographed, MRS

WT generated the tRNA-bound complex in a dose-dependent manner, whereas the MRS S662D mutant did not bind tRNA (Figure I-9A). When the same reaction mixtures were tested by dot blot analysis, similar results were observed (Figure I-9B). If the MRS S662D mutant cannot bind tRNA, it would not be able to produce Met-tRNA^{Met}. As expected, the MRS S662D mutant showed negligible aminoacylation activity in contrast to MRS WT (Figure I-9C). The reduced activity of the MRS S662D mutant was not due to nonspecific amino acid substitution since the MRS S662A mutant still showed its activity.

Given that UV-dependent MRS phosphorylation blocks the charging ability of MRS, the level of Met-tRNA^{Met} should be reduced by UV treatment. Indeed, decreased levels of Met-tRNA^{Met} were observed in the UV-treated cells by autoradiography (Figure I-9D left and middle). Under the same conditions, the UV-irradiated cells showed decreased global protein synthesis (Figure I-9D right). The UV-dependent reduction of Met-tRNAi^{Met} was also confirmed in GCN2 MEFs and HeLa cells by Northern blotting (Figure I-10A and B). To test whether phosphorylation of MRS at Ser662 would affect global translation, I introduced MRS WT and the S662D mutant into HeLa cells and selected two independent stable cell lines expressing MRS WT or the S662D mutant. To remove any contribution from endogenous MRS, I designed si-RNA targeting the 3′UTR sequence of endogenous MRS transcript and specifically suppressed

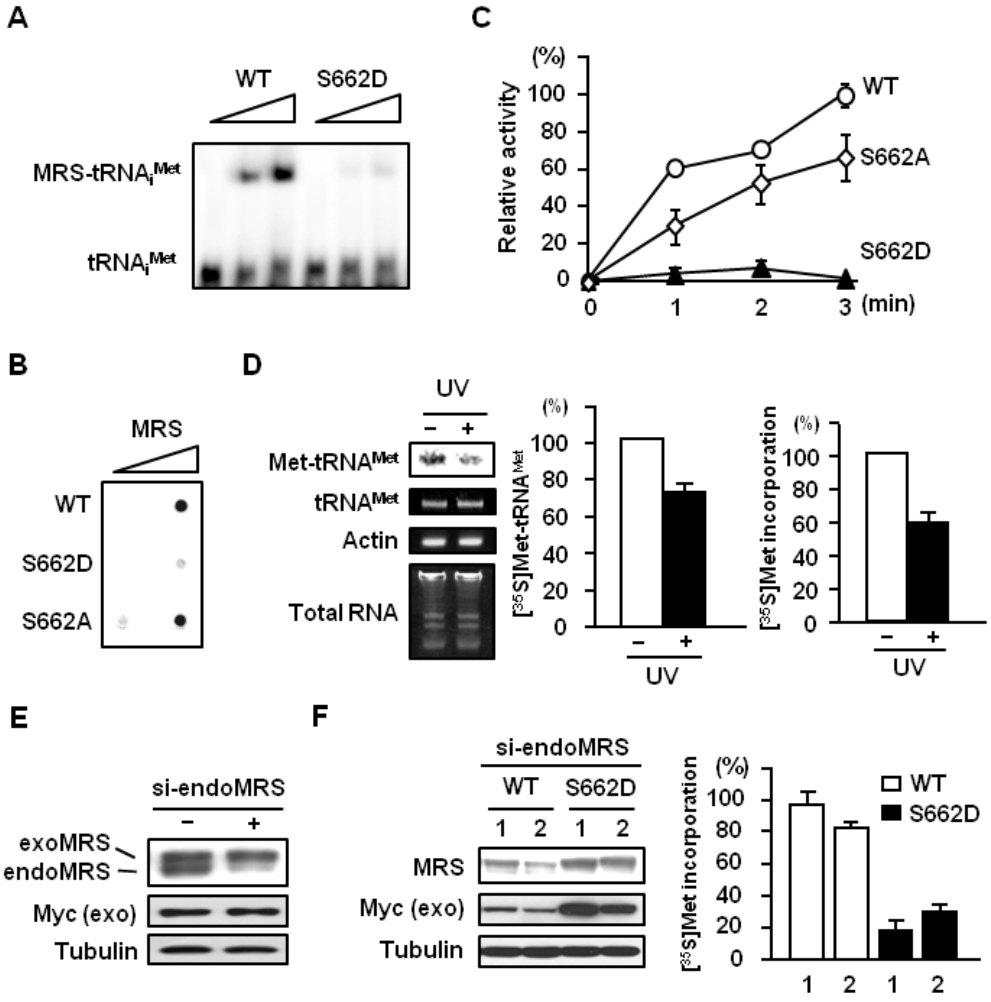

Figure I-9. The effect of MRS phosphorylation on tRNA binding and global translation. (A and B) The [α-^{32}P]UTP-incorporated tRNA$_i^{Met}$ probe was incubated with His-MRS WT and S662D proteins and separated by non-denaturing PAGE **(A)** or filtered through a nitrocellulose membrane **(B)**. Bound tRNAs were detected by autoradiography. **(C)** Relative catalytic activities of His-MRS WT and mutants were assessed by aminoacylation assay. Data are represented as mean +/− SD (n = 3). **(D)** HeLa cells were incubated with [^{35}S]methionine for 45 min with or without UV irradiation. Total RNA extracted under acidic conditions was run by acid urea PAGE.

Charged $tRNA^{Met}$ was detected by autoradiography (D, left panel), and the relative Met-$tRNA^{Met}$ amount was quantified by digital imaging (D, middle). The values are represented as mean +/− SD (n = 2). Protein synthesis under the same conditions was monitored by the [^{35}S]methionine incorporation assay (D, right). Data are represented as mean +/− SD (n = 3). **(E)** Stable HeLa cells expressing Myc-tagged MRS WT were transfected with si-RNA specific to the 3′UTR of MRS mRNA. After 72 h incubation, MRS levels were detected by immunoblotting with specific antibodies. Endogenous MRS was effectively knocked down by 3′UTR-specific si-RNA treatment, while exogenous MRS was not affected. **(F)** Endogenous MRS was downregulated in MRS WT and S662D stable HeLa cells by si-RNA treatment for 72 h (left). Stable cell clones were starved in methionine-free media for 30 min following incubation with [^{35}S] methionine for 1 h and assayed for global translation. Data are represented as mean +/− SD (n = 3) (right).

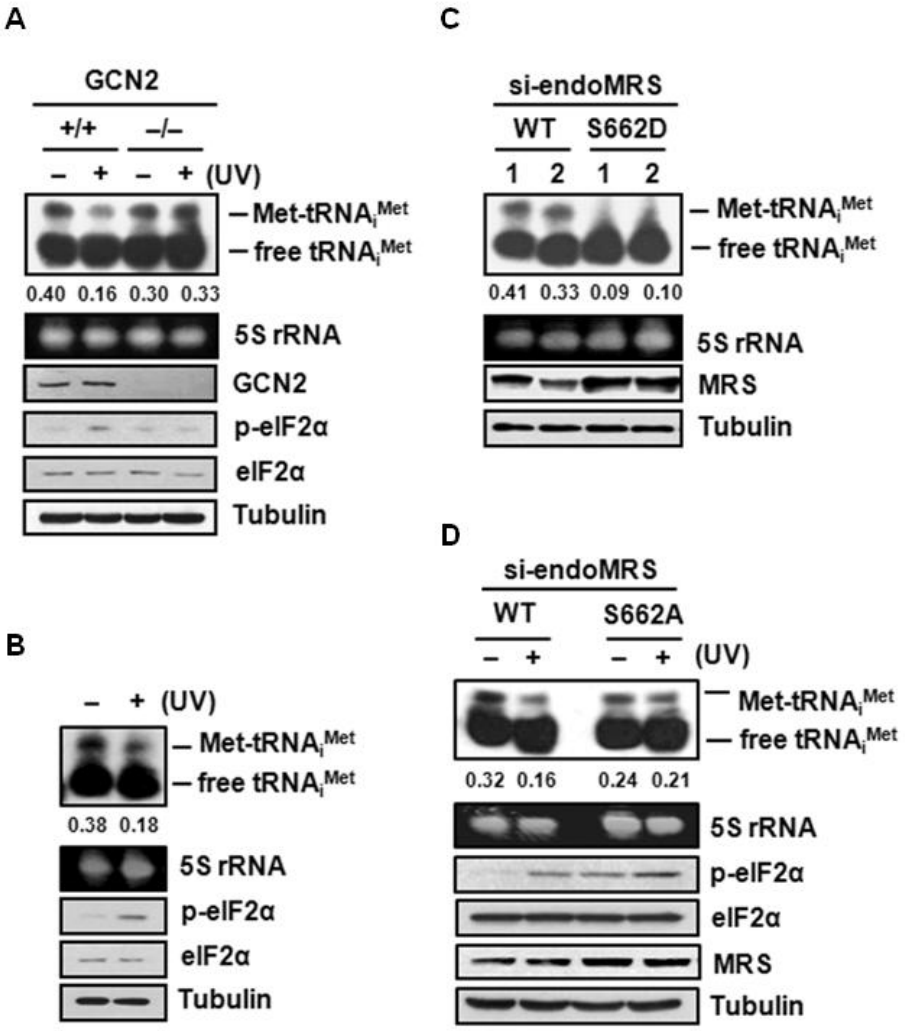

Figure I-10. The analysis for the charged initiator tRNA. Levels of charged tRNAi^{Met} in UV-irradiated GCN2 mouse embryonic fibroblasts **(A)** or HeLa **(B)** were analyzed by acid-gel urea PAGE and Northern blotting. rRNA was used as a loading control. **(C)** Stable HeLa cells expressing MRS WT or the MRS S662D mutant were treated with 3' UTR targeted-siRNA specific to endogenous MRS, and levels of charged tRNAi^{Met} were detected by acidic PAGE and Northern blotting. **(D)** After endogenous MRS was knocked down, stable cells expressing MRS WT or the MRS S662A mutant were UV-irradiated and analyzed for the levels of charged Met-tRNAi^{Met}.

Elevated p-eIF2α in the S662A-expressing cells implies that translational control via eIF2α could be enhanced when p-MRS–mediated translation control is not available, perhaps as a compensatory mechanism. The relative ratio of charged initiator tRNA to free initiator tRNA was quantified and presented.

the expression of endogenous MRS, while not affecting exogenous MRS (Figure I-9E). Endogenous MRS was knocked down in the stable HeLa cell lines (Figure I-9F left) and I compared the global translation between these cell lines and found that protein synthesis in cells expressing the MRS S662D mutant was reduced to about 20% of that in cells expressing MRS WT (Figure I-9F right). Cells expressing the MRS S662D mutant showed little amounts of Met-tRNAi^{Met} with knockdown of endogenous MRS (Figure I-10C). In the same context, portions of charged tRNAi^{Met} were reduced by UV stress in stable cells where ectopic MRS WT was substituted for endogenous MRS; however, it was not observed in stable cells expressing the MRS S662A mutant (Figure I-10D). These data suggest that phosphorylation at Ser662 in MRS not only trigger the release of AIMP3 for nuclear translocation but also downregulates global translation by blocking binding with tRNA substrate to MRS.

MRS and eIF2α cooperate in controlling protein synthesis following UV irradiation

UV-activated GCN2 is known to phosphorylate eIF2α at Ser52 (Ser51 in mouse), which induces a global translation block via inhibition of the TC formation (22). Since MRS is an additional substrate of GCN2 and can also work for translational inhibition upon UV stress, I investigated whether there is a potential

crosstalk between the two pathways. First, I knocked down either MRS or eIF2α. Second, I generated the cell lines stably overexpressing either the MRS S662A or the eIF2α S52A mutants that are not phosphorylated by GCN2. In these two systems, I checked how the inactivation of each pathway would affect the counterpart. I observed that UV-induced phosphorylation of MRS was elevated when eIF2α was suppressed (Figure I-11A). Conversely, suppression of MRS enhanced p-eIF2α by UV irradiation (Figure I-11B). Likewise, stable overexpression of the eIF2α S52A mutant, which serves as a dominant-negative, adversely affected endogenous p-eIF2α production, and enhanced UV-induced phosphorylation of MRS (Figure I-11C). HeLa stable cell lines which expressing the MRS S662A mutant also showed increased level of p-eIF2α compared to stable cells expressing MRS WT (Figure I-11D). Disassociation of AIMP3 from MRS following UV irradiation was observed in all the experimental conditions except when the MRS S662A mutant was immunoprecipitated for the analysis of bound AIMP3 . It demonstrates that phosphorylation of MRS at Ser662 is the real prerequisite step for AIMP3 release. Knockdown or overexpression of each protein did not affect total protein level of the counterpart, overall. These data suggest that level of p-eIF2α and p-MRS could be controlled complementarily to each other. To see the contribution of both proteins on the global translation regulation, [^{35}S]methionine incorporation assay was conducted using stable

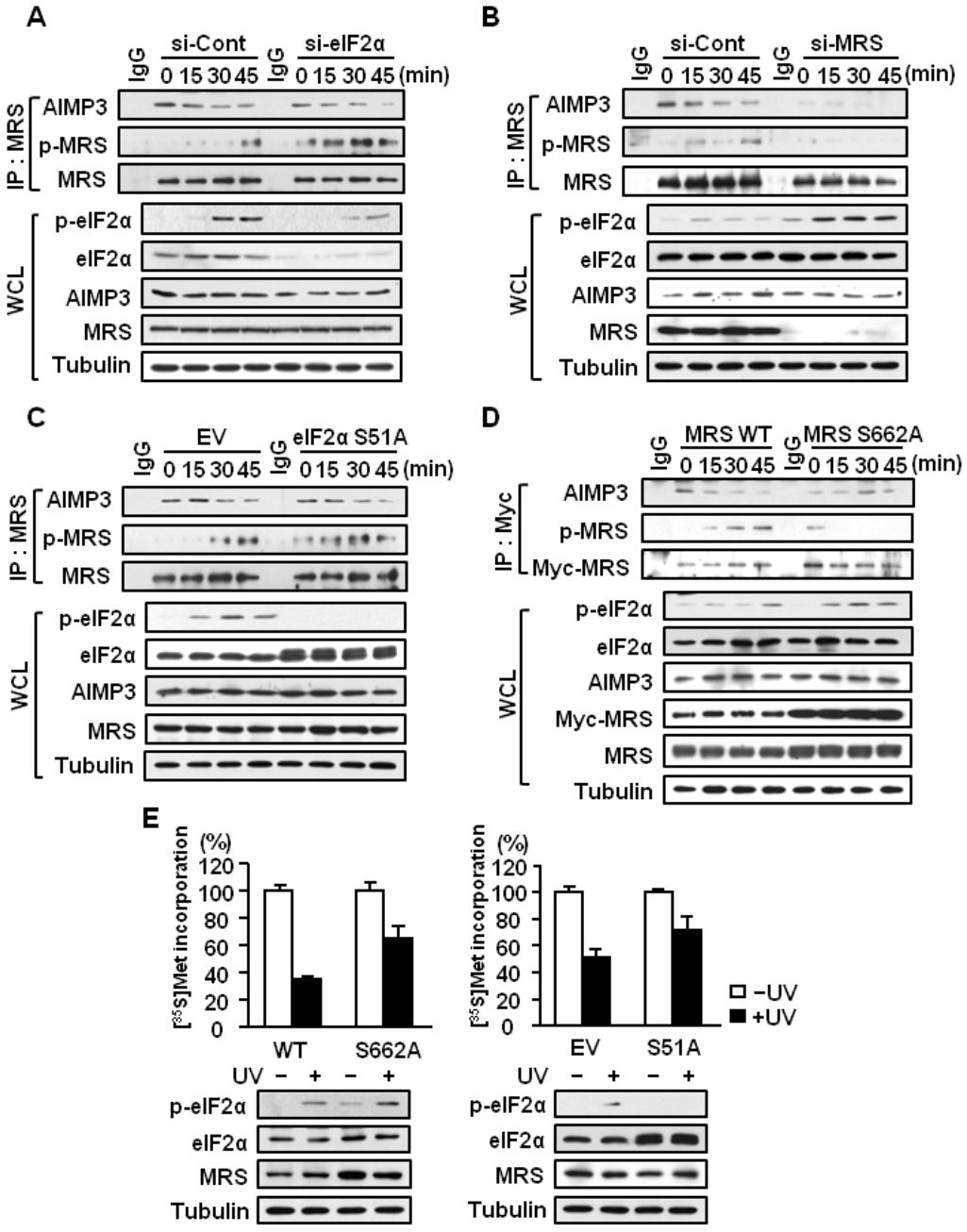

Figure I-11. MRS coordinates with eIF2α to regulate translation upon UV irradiation. (A and B) HeLa cells treated with si-RNA specific to eIF2α or MRS were

irradiated by UV and phosphorylation of MRS and eIF2α was monitored. Phosphorylation of MRS was more enhanced in eIF2α-knockdown cells **(A)** and p-eIF2α was more elevated in MRS-knockdown cells **(B)** compared to control cells. **(C and D)** UV-induced phosphorylation of MRS and eIF2α was monitored in stable cell lines expressing the eIF2α S52A or MRS S662A mutant. More intense p-MRS was observed when eIF2α is unphosphorylatable **(C)**. The eIF2α S52A mutant, tagged by Myc, migrated slowly and appeared in upper band of endogenous eIF2α. Phoshorylation of eIF2α was more increased in cells expressing the MRS S662A mutant compared to control cells expressing MRS WT **(D)**. **(E)** Protein synthesis after UV irradiation was measured with stable cells expressing MRS WT and the S662A mutant (left) and EV and the eIF2α S52A mutant (right) by methionine incorporation. Endogenous MRS in cells expressing MRS WT and the S662A mutant was knocked down by si-RNA treatment. Stable cell lines were incubated with [^{35}S]methionine for 45 min with or without UV irradiation and radioactivity incorporated into synthesized proteins were countered. Partial recovery of translation was observed in cells expressing nonphosphorylatable MRS or eIF2α mutants compared to control cells.

HeLa cells expressing the MRS S662A or the eIF2α S52A mutant. Protein synthesis in MRS WT cells was reduced to about 33% by UV stress whereas that in the cells expressing the MRS S662A mutant was only decreased to 65% (Figure I-11E left). Similar result was obtained from the stable cells expressing the eIF2α S52A mutant which showed 26% decrease of protein synthesis while it was reduced to 55% in control cells (Figure I-11E right). According to the results, MRS and eIF2α seem to cooperate for efficient controlling of translation upon UV stress. Phosphorylation of each protein could be augmented when the other counterpart is functionally uncontrolled and dual phosphorylation of MRS and eIF2α can inhibit translation more effectively. Phosphorylation of MRS can block new Met-tRNA^{Met} production while p-eIF2α inhibits the TC formation with pre-existing Met-tRNA$_i^{Met}$. In conclusion, GCN2-induced phosphorylation of MRS links translation regulation and DNA damage response via release of AIMP3 which is translocated into nucleus and involved in p53-dependent DNA damage response (Figure I-12).

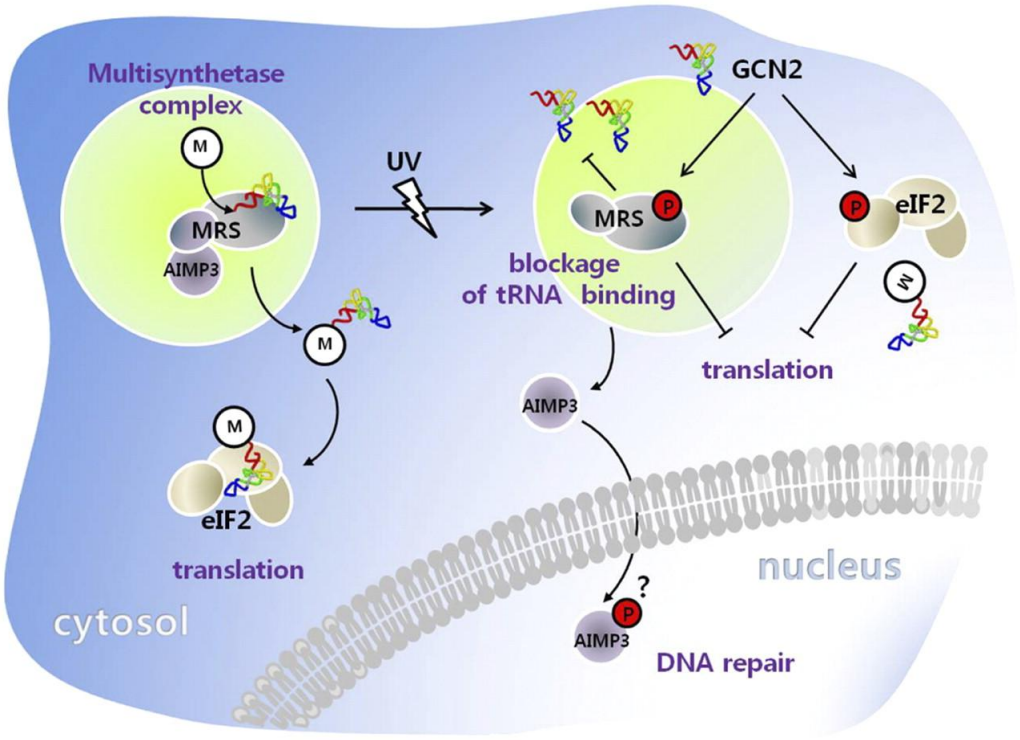

Figure I-12. Schematic representation showing the dual role of MRS. GCN2-dependent MRS phosphorylation affects on tRNA and AIMP3 binding. Under normal conditions, MRS catalyzes aminoacylation of $tRNA^{Met}$ for translational initiation. AIMP3 stays bound to the N-terminal extension of MRS. Upon UV irradiation, MRS is phosphorylated at Ser662 by GCN2, which then blocks the binding of $tRNA^{Met}$. Phosphorylation of MRS induces a conformational change leading to the dissociation of AIMP3 from MRS. Released AIMP3 is translocated into nucleus for the repair of damaged DNA. GCN2 also phosphorylates eIF2α and p-MRS and p-eIF2α work together for the control of global translation.

DISCUSSION

UV-activated GCN2 is known to phosphorylate eIF2α at Ser52, which induces a global translation block via inhibition of the TC formation (22). Here, I report that MRS is an additional GCN2 substrate that can work with eIF2α for translational regulation upon UV-induced stress. Interestingly, the influence of MRS phosphorylation upon UV irradiation was not restricted to translation control. MRS linked translational block to DNA damage response by regulating molecular interaction with tumor suppressor AIMP3.

Phosphorylation of MRS by GCN2 made AIMP3 free for nuclear translocation. The disassociation between MRS and AIMP3 was dramatic as observed in BiFC analysis (Figure I-2B). The decrease of AIMP3 in cytosol, however, was not distinct, while increase of AIMP3 in nucleus was clearly detected (Figure I-2E). Considering that almost all amounts of protein samples obtained from nuclear fraction were analyzed for the immunoblotting in contrast to those from cytosol, it seems reasonable that the change of AIMP3 could be only detected in nucleus. Still and all, there is a gap between the amount of released AIMP3 and relocalized AIMP3. This discrepancy suggests that all the AIMP3 released from MRS are not translocated into nucleus. AIMP3 might be subjected to a process of modification for the nuclear localization, although

AIMP3 should be released from MRS first. To test the possibility of AIMP3 modification, I fractionated methionine-starved and $tRNA_i^{Met}$-overexpressed cells. In these cells, MRS is phosphorylated without DNA damage, which augments the levels of free AIMP3. If further AIMP3 modification is not necessary for translocation, nuclear AIMP3 levels in these cells after UV irradiation should remain unchanged, and similarly, elevated nuclear AIMP3 levels should occur in the absence of UV irradiation. However, UV-dependent nuclear translocation of AIMP3 was observed and basal nuclear AIMP3 was not elevated (Figure I-13A and B). It suggests the possibility of post-translational modification of free AIMP3. I found that phosphorylation is a possible modification, based on the 2D-PAGE analysis of nuclear AIMP3 (Figure I-13C). Although the exact kinase and phosphorylation site(s) for AIMP3 is not proved yet, it implies that coupling of translation control to DNA damage response is a complex step and needed sequential modification of related counterparts. AIMP3 itself is functionally versatile. In addition to its tumor suppressive activity, increase in cellular AIMP3 levels was recently shown to enhance cellular senescence via negative regulation of lamin A (30). Considering its diverse roles, it is plausible that AIMP3 is subject to multiple post-translational modifications for the control of its activities. The additional role of AIMP3 in cytosol and its post-translational modifications should be studied further.

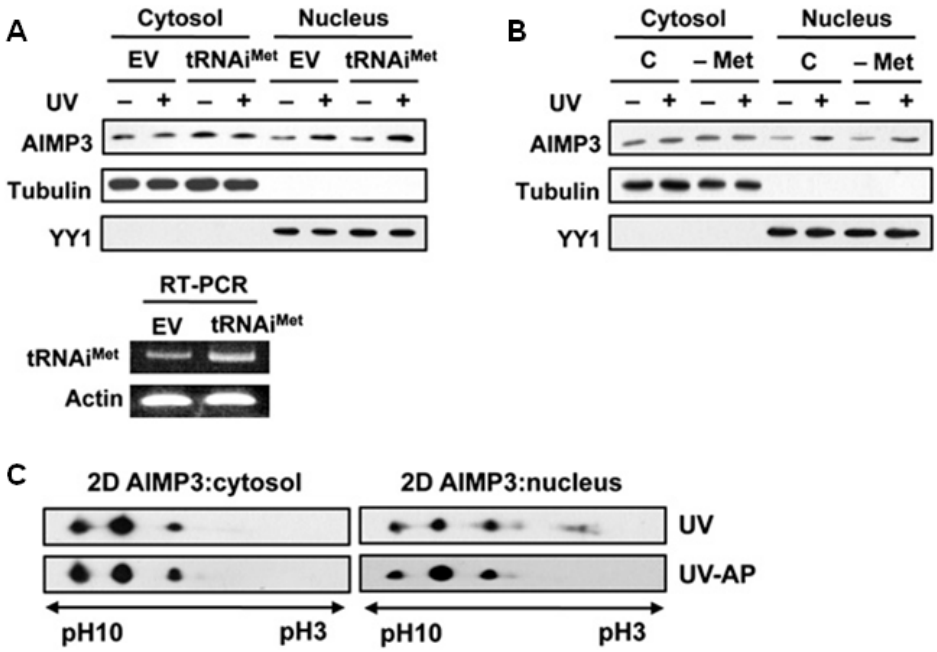

Figure I-13. Posttranslational modification of AIMP3 is needed for nuclear translocation. (A) HeLa cells transfected with initiator tRNA were UV-irradiated, and cytosol and nucleus were prepared from UV irradiated-HeLa cells. Nuclear AIMP3 was analyzed by immunoblotting. EV-transfected cells were used as a control. **(B)** HeLa cells starved with methionine for 1 h were irradiated by UV and fractionated for the analysis of nuclear AIMP3 by immunoblotting. Untreated cells were used as a control. **(C)** UV-irradiated HeLa cells were fractionated and analyzed by 2D-PAGE. Shift of protein spots to the acidic side, disappeared by alkaline phosphatase (AP) treatment was observed in nucleus. AIMP3 could be phosphorylated in nucleus but not in cytosol.

GCN2 also appears to be involved in control of AIMP3 and MRS expression. In *GCN2*$^{-/-}$ MEFs, bound AIMP3 to MRS was basally low in the absence of UV (Figure I-4B). This effect appears related to reduced expression of MRS and AIMP3, specifically AIMP3, in the *GCN2*$^{-/-}$ MEFs. Interestingly, among the translation-related proteins tested in this study, only the levels of MRS and AIMP3 were reduced by the absence of GCN2 (Figure I-14). In contrast, when GCN2 was transiently suppressed by siRNA, MRS and AIMP3 levels were little affected (Figure I-4A). Perhaps, in *GCN2*$^{-/-}$ cells constitutively lacking the GCN2 activity, a risk of uncontrolled translation may be compensated by reducing cellular levels of MRS and AIMP3, although the precise role of GCN2 in this connection is currently unknown.

There are several examples of the dynamic relationship of MSC components being controlled by phosphorylation. For instance, EPRS, the largest component of the complex, dissociates from the complex in IFN-γ-activated U937 cells and forms a new multi-component complex called IFN-γ-activated inhibitor of translation (GAIT) with the 3′UTR of the target transcripts for translational gene silencing (31). In addition, lysyl-tRNA synthetase (KRS) is phosphorylated in mast cells for nuclear localization where it controls the activity of microphthalmia transcription factor, MITF (32). Among 3 non-enzymatic components, AIMP1, AIMP2, and AIMP3, AIMP2 was shown to be

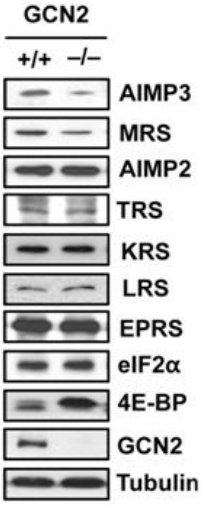

Figure I-14. Expression of translation-related proteins in GCN2 mouse embryonic fibroblasts. Expression level of several translational components was analyzed by westernblotting. The protein level of MRS and AIMP3 affected by GCN2 knockdown.

phosphorylated, which promoted translocation of AIMP2 in nucleus where it bound p53 upon DNA damage (33). MRS phosphorylation can be distinguished from these cases: Phosphorylated MRS is not dissociated from MSC but instead releases bound AIMP3 and phosphorylation of MSC components has not been previously shown to affect global translation. Here, I found that phosphorylation significantly suppresses the catalytic activity of MRS, leading to downregulation of global translation. This finding provides the evidences showing a unique role of MRS as a coordinator of cytosolic translation and nuclear DNA repair process.

MRS primarily recognizes its substrate tRNA through interaction with the anticodon. Since the GCN2-dependent phosphorylation site is located within the C-terminal anticodon-binding domain (Figure I-1A), phosphorylation may result in steric hindrance and charge repulsion for the docking of $tRNA^{Met}$ to the anticodon-binding domain, leading to the reduction of the catalytic capability of MRS. The C-terminal domain of MRS is expected to be exposed to interact with $tRNA^{Met}$ and GCN2. Phosphorylation at Ser662 in the C-terminal domain of MRS appears to induce a long-range conformational change, reducing the interaction of the N-terminal extension with AIMP3.

GCN2 is known to be activated by uncharged tRNAs which bind Histidyl- tRNA synthetase (HRS) region of GCN2 (22). The exact mechanism of GCN2 activation by UV has not been solved yet and any evidence for

deacylation of tRNAs in UV-treated cells was not reported. The most probable model for GCN2 activation by UV is the induction of crosslinking between GCN2 and tRNAs (22). In this study, tRNA damage in cytosol seems to be recognized as a signal for DNA damage in nucleus. Considering that translation block and DNA damage response should occur in early time points following UV irradiation, tRNA-mediated signal transduction is a timely relevant strategy in that tRNAs are ubiquitous and plenty to sense any nucleic acids damage signals promptly. As MRS phosphorylation links UV stress to the DNA damage response via AIMP3 translocation, eIF2α phosphorylation increases the NF-κB response upon UV irradiation (26). While AIMP3 release from MRS and nuclear translocation was observed within 1 hr after UV irradiation, NF-κB activation by eIF2α phosphorylation is observed at least 1 hr after UV irradiation (26). It implies that GCN2-mediated phsosphorylation of MRS and eIF2α team up not only for translation control but also for DNA damage-cell cycle check point. GCN2 may use MRS-AIMP3 as an early response to UV-induced DNA damage and eIF2α for the transcriptional control of NF-κB-dependent genes in later stages of DNA damage. GCN2-mediated delay in cell cycle entry into S phase by UV stress has been reported, however the underlying mechanism and crosstalk between GCN2 and ATM/ATR in cell cycle regulation and DNA repair are not clearly understood (34). This work suggests that GCN2 can indirectly

activate ATM/ATR via AIMP3 released from phosphorylated MRS, although the concise relationship among ATM/ATR, NF-κB, p-eIF2α, and AIMP3 remains to be answered. In conclusion, I demonstrated dual roles of human MRS in the regulation of cytosolic translation and molecular interaction with AIMP3, coupling control of protein synthesis to DNA damage response. The significance of this work can be also seen from the point that MRS is suggested as a new gate for translational control, posing a possibility that other ARSs may play roles in their unique ways to control translation as well as cell signaling.

MATERIALS AND METHODS

Cell Culture

$GCN2^{+/+}$ and $GCN2^{-/-}$ MEFs, HeLa, and 293T cells were grown in Dulbecco's modified Eagle's medium supplemented with 10% serum and 1% penicillin/streptomycin in 5% CO_2 at 37℃. For the selection of stable cell line, myc-MRS wild type and mutant were transfected with FuGENE HD (Roche) in HeLa cells. After selection with 1 mg/mL geneticin (G418, Duchefa Biochemie), stable cells were maintained with 1 mg/mL G418. Transfections with siRNA were performed using Lipofectamine 2000 (Invitrogen). For IP or immunofluorescence (IF) assay, cells were UV-irradiated (60 J/m^2) and recovered with serum-free (SF) medium.

Antibodies

Antibodies for tubulin (mouse, Sigma), Flag (mouse, F3156, Sigma), Myc (mouse, sc-40, Santa Cruz), YY1 (mouse, sc-7341, Santa Cruz), eIF2α (rabbit, sc-11386, Santa Cruz), p-eIF2α (rabbit, #9721S, Cell Signaling), GCN2 (rabbit, ab70214, Abcam), p-GCN2 (rabbit, #3301, Cell Signaling), p-Serine (rabbit, ab9332, Abcam) and p-Threonine (rabbit, #9381, Cell Signaling) were used to carry out western blot, immunoprecipitation, and immunofluorescence assays.

Antibodies for MRS, EPRS, and AIMP3 were previously described (6). Polyclonal rabbit antibody specific to p-Ser662 of MRS was produced using synthetic peptide containing p-Ser662 (GMFV{pSer}KFFGGYVPEC) as an immunogen (Genscript).

Cloning and Detection of $tRNA_i^{Met}$ and $tRNA_e^{Met}$, and Small Interference RNA (siRNA) Sequences

Human genomic DNA sequences around $tRNA_i^{Met}$ and $tRNA_e^{Met}$ were PCR-amplified with primer pairs, 5′-AAAGTGCAGTGACTACAGGCGTGA-3′ and 5′-ATGACACTTGGGTGTCCATGA-3′ for $tRNA_i^{Met}$ and 5′-TTGACCCTGGG-TTTGTTCCTGTGA-3′ and 5′-TACACGTGCTCTTTCCTGGACACT-3′ for $tRNA_e^{Met}$, and cloned into the pGEM-T-Easy vector (Promega). Primers for RT-PCR and DNA probes were 5′-CTGGGCCCATAACCCAGAG-3′ and 5′-TGGT-AGCAGAGGATGGTTTC-3′ for $tRNA_i^{Met}$, and 5′-CTCGTTAGCGCAGTAGG-TAGC-3′ and 5′-GGATCGAACTCACGACCTTC-3′ for $tRNA_e^{Met}$, respectively. Sequences of siRNAs specific to GCN2 and the 3′UTR of endogenous MRS were 5′-GCAUAAGGUCCUGAGUGCAUCUAAU-3′ and 5′-UUUAUUACU-GUCCCUAUCU-3′, respectively.

Immunoprecipitation (IP) Assay

Cells were lysed with immunoprecipitation (IP) buffer (50 mM Tris-HCl pH 7.4, 150 mM NaCl, 0.5% Triton X-100, 5 mM EDTA, and 10% glycerol) containing protease inhibitor and phosphatase inhibitor. Cell lysates were centrifuged and incubated overnight with normal IgG or specific antibodies and then with Protein A/G agarose. Immunoprecipitated proteins were separated by SDS-PAGE and detected by immunoblotting.

***In vitro* Pull-Down Assay**

GST- and MBP-fusion proteins were expressed in *Escherichia. coli* BL21 (DE3) and induced with 1 mM isopropyl-β-D-thiogalactopyranoside (IPTG) for 6 h at 30℃. Harvested cells were lysed by sonication, and lysates were incubated with glutathione sepharose 4B (GE Healthcare) or amylase resin (New England BioLabs) in lysis buffer (1X PBS containing 0.5% Triton X-100, 1mM DTT, 1mM EDTA and protease inhibitor). Radiolabelled AIMP3 and MRS were synthesized by *in vitro* translation with the TNT-coupled translation kit (Promega) and incubated with immobilized GST- or MBP-fusion protein. Eluted proteins were separated by SDS-PAGE and detected by autoradiography.

Yeast Two-Hybrid Assay

Full-length (F) and deletion domains (D) of MRS and AIMP3 were cloned into

pLexA and pJG4-5 (B42). LexA- and B42-fusion proteins (LexA-MRS F and B42-AIMP3 Ds or LexA-AIMP3 F and B42-MRS Ds) were expressed in the yeast strain EGY/SH. Interactions were determined by induction of reporters, LEU2, and lacZ. To detect interactions, colonies were picked and streaked onto Ura^-, His^-, Trp^-, Leu^-/glucose media and Ura^-, His^-, Trp^-/galactose media containing X-gal and raffinose.

Bimolecular Fluorescence Complement and Immunofluorescence Assays

AIMP3 and MRS were cloned into pBiFC-VN173 (Flag tag) and pBiFC-VC155 (HA tag). HeLa cells were co-transfected with the pBiFC-VN173-AIMP3 and pBiFC-VC155-MRS. Next day, the cells were UV-irradiated (60 J/m^2) and recovered with SF medium. These cells were fixed with 100% methanol for 15 min at room temperature (RT) and incubated with blocking solution (PBS containing 1% bovine serum albumin and 0.05% Triton X-100) for 1 h at RT. After blocking, the cells were stained with primary antibody and Alexa555-conjugated secondary antibody for 1 h. DAPI was used for nuclear staining. HeLa cells transfected with pEGFP-AIMP3 were UV-irradiated and recovered with SF medium. At various time points, the cells were harvested, fixed, and stained with PI. After mounting, MRS and AIMP3 interaction and cellular localization of AIMP3 was observed by fluorescence and confocal microscopy.

Cell Fractionation

HeLa cells were UV-irradiated and recovered with SF medium. After harvest, irradiated cells were lysed with buffer A (10 mM HEPES pH 7.4, 10 mM KCl, 100 µM EDTA, 1 mM DTT, 0.4% NP-40, and protease inhibitor cocktail). Cell lysates were centrifuged at 15,000 *g* for 3 min, and the supernatants were transferred into a new tube. The pellets were washed twice with 1× cold PBS and resuspended in buffer B (10 mM HEPES pH 7.4, 400 mM NaCl, 1 mM EDTA, 1 mM DTT, 10% Glycerol, and protease inhibitor cocktail). After incubation for 1 h, the re-suspensions were centrifuged at 15,000 *g* for 5 min to obtain the nuclear fraction.

Two-Dimentional Polyacrylamide Gel Electrophoresis (2D-PAGE)

Phosphorylation detection with 2D-PAGE was carried out as previously described (33). Briefly, proteins were rehydrated in re-solubilisation buffer (7 M urea, 2 M thiourea, 2% ASB-14, 0.5% Triton X-100, 1% ampholyte, 1% tributylphosphine, and 0.1% bromophenol blue). Protein solutions were absorbed into 7-cm pH-gradient strips and subjected to isoelectric focusing.

***In Vitro* Kinase Assay**

MBP-fusion MRS deletion domains D1 (residues 1–266), D2 (267–597), and D3

(598–900) were purified from *Escherichia coli* BL21 (DE3) using amylose resin. Flag-GCN2 expressed in 293T cells was immunoprecipitated and incubated with each purified MBP-MRS domain in kinase buffer (20 mM Tris-HCl pH 7.4, 50 mM NaCl, 10 mM $MgCl_2$, 1 mM DTT, 250 μM ATP, and 10 μCi [γ-^{32}P]ATP) at 30℃. For the peptide kinase assay, N-terminal biotinylated peptides were chemically synthesized (GL Biochem) and GST-GCN2 kinase domain (KD) WT and the K618R mutant expressed from E. coli BL21 (DE3) were immobilized with glutathione Sepharose 4B beads. Each peptide [25 μM of MRS Ser662 (RAGMFVSKFFGG), MRS S662A (RAGMFVAKFFGG), GCN2 Thr899 (PSGHLTGMVGT), and eIF2α Ser52 (ELSRRRIR)] was reacted with the GST-GCN2 kinase domain at 30℃ for 30 min. Reaction mixtures were filtered through a streptavidin-coated matrix biotin-capture membrane (35) using a 96-well Minifold filtration apparatus. Phosphorylated peptides were detected by autoradiography.

Nano-LC-MS/MS Analysis

Protein bands cut from SDS-PAGE gels were trypsin digested, and nano-LC-MS/MS analysis was performed on an Agilent 1100 series nano-LC and LTQ-mass spectrometer (Thermo electron).

Northern Blotting for $tRNA^{Met}$ Detection

Total RNA (30 μg), isolated with the miRNeasy Mini Kit (Qiagen), was separated by 6.5% urea (8%) PAGE and transferred onto a nylon membrane with a semi-dry transfer apparatus. DNA probes were PCR-amplified and biotinylated with the BrightStar Psoralen-Biotin kit (Ambion). Northern hybridization was performed using the BrightStar BioDetect kit (Ambion). For the analysis of charged tRNA, total RNA was run by acid-gel urea PAGE and subjected to Northern hybridization using initiator tRNA-specific probe (36).

Coexpression and Copurification of AIMP3 and MRS

AIMP3 gene was cloned into the His-tag multiple cloning site (MCS) of pACYCDuet (Novagen) to construct pKMJ101. The MRS gene was cloned into the S-tag MCS of pKMJ101 to construct pKMJ102. Site-directed mutagenesis was used to introduce the S662D mutation into pKMJ102. pKMJ101, pKMJ102, and pKMJ103 (the MRS S662D mutant) were transformed into *E. coli* BL21 (DE3), and His-AIMP3 was purified using Ni-NTA agarose. Co-purification of MRS WT and the S662D mutant was confirmed by immunoblotting.

Circular Dichroism (CD) Spectrum

MBP-fusion MRS WT and S662D mutant were purified using amylase resin.

MBP-tag proteins, eluted with lysis buffer containing 50 mM maltose at 4℃ overnight, were dialyzed with 10 mM potassium phosphate buffer (pH 7.4). The CD spectrum was analyzed with a Jasco J-815 CD spectrometer at 25℃ in the range of 250–350 nm. Samples were loaded into a 0.1-cm path-length cuvette. The results are presented as an average of three repeated scans after subtraction of buffer background.

Protein Digestion by Trypsin and Elastase

MBP-MRS WT and the S662D mutant (15 μg) were digested with 5 μg trypsin (HyClone) for 3 min at RT or 0.6 U of elastase (Sigma) for 30 min at 37℃. Digested samples were separated by SDS-PAGE and stained with Coomassie brilliant blue.

Insertion of Peptide Linker (PL)

Insertion of the peptide linker (PL) with the sequence of Gly-Gly-Gly-Gly-Ser between the residues 233 and 234 of MRS WT and of the S662D mutant was performed with the QuickChange site-directed mutagenesis kit (Stratagene). Primer pairs, 5′-TCTGAGGAGGAGATTGGCGGCGGCGGCTCTGCTATGG-CTGTTACT-3′ and 5′-AGTAACAGCCATAGCAGAGCCGCCGCCGCCAAT-CTCCTCCTCAGA-3′ were used for the mutational insertion into pGEX-4T-1

encoding MRS WT or the MRS S662D mutant.

Gel Shift and Filter Binding Assays

Initiator $tRNA^{Met}$ was synthesized by *in vitro* transcription with [α-^{32}P]UTP (3000 Ci/mmol, Izotop). Purified His-MRS proteins were mixed with the $tRNA_i^{Met}$ probes in the binding buffer (20 mM Tris-HCl pH 7.4, 75 mM KCl, 10 mM $MgCl_2$, and 5% glycerol) and incubated at 30℃ for 30 min. Reaction mixtures were separated by 6% nondenaturing PAGE and dried. For the dot blot assay, reaction mixtures were filtered through a nitrocellulose membrane using a 96-well Minifold filtration apparatus.

Aminoacylation Assay

His-tagged MRS expressed in *E. coli* Rosetta (DE3) was purified using ProBond^{TM} Resin (Invitrogen), following washing with lysis buffer containing 20 mM KH_2PO_4 and 500 mM NaCl, pH 7.8 and with lysis buffer containing 10% glycerol and then changing the pH from 7.8, to 6 and 5.2, and back to 6 using 20 mM imidazole at the final step. His-MRS was eluted in the presence of 200 mM imidazole (pH 6.0) and dialyzed with PBS containing 20% glycerol. Initiator $tRNA^{Met}$ was synthesized by *in vitro* transcription. MRS aminoacylation activity was assayed at 37℃ in reaction buffer (30 mM HEPES, pH 7.4, 100

mM potassium acetate, 10 mM magnesium acetate, 2 mM ATP, 20 µM methionine, 100 µg/mL $tRNA_i^{Met}$, and 25 µCi [^{35}S]methionine (1000 Ci/mmol, Izotop). Aminoacylation reactions were quenched on 3MM filter paper pre-wetted with 5% trichloroacetic acid (TCA) containing 1 mM methionine. After washing with 5% TCA and drying, radioactivity was detected by liquid scintillation counter (Wallac 1409).

Radiolabelled Met-$tRNA^{Met}$ Isolation

Cells were incubated in methionine-free media with 1 µCi [^{35}S]methionine (1175 Ci/mmol, Perkin Elmer) for 30 min. Total RNA (30 µg) was purified under acidic conditions, and Met-$tRNA^{Met}$ was detected as described previously (36).

[^{35}S]methionine Incorporation Assay

Cells were incubated in methionine-free media containing 1 µCi [^{35}S]methionine. After incubation, the cells were washed with cold PBS, and the amount of radioactive protein was measured by liquid scintillation. Count data were normalized to cell number.

REFERNCES

1. Gebauer, F., Hentze, M. W. (2004) Molecular mechanisms of translational control. Nat. Rev. Mol. Cell Biol. **5,** 827-835

2. Pavon-Eternod, M., Gomes, S., Geslain, R., Dai, Q., Rosner, M. R., and Pan, T. (2009) tRNA over-expression in breast cancer and functional consequences. Nucleic Acids Res. **37,** 7268-7280

3. Sonnenberg, N., and Hinnebusch, A. G. (2009) Regulation of translation initiation in eukaryotes: mechanisms and biological targets. Cell **136,** 731-745

4. Lee, S. W., Cho, B. H., Park, S. G., and Kim, S. (2004) Aminoacyl-tRNA synthetase complexes: beyond translation. J. Cell Sci. **117,** 3725-3734

5. Park, S. G., Ewalt, K. L., and Kim, S. (2005) Functional expansion of aminoacyl-tRNA synthetases and their interacting factors: new perspectives on housekeepers. Trends Biochem. Sci. **30,** 569-574

6. Ko, Y. G., Kang, Y. S., Kim, E. K., Park, S. G., and Kim, S. (2000) Nucleolar localization of human methionyl-tRNA synthetase and its role in ribosomal RNA synthesis. J. Cell Biol. **149,** 567-574

7. Netzer, N., Goodenbour, J. M., David, A., Dittmar, K. A., Jones, R. B., Schneider, J. R., Boone, D., Eves, E. M., Rosner, M. R. Gibbs, J. S., Embry, A., Dolan, B., Das, S., Hickman, H. D., Berglund, P., Bennink, J. R., Yewdell, J. W., and Pan, T. (2009) Innate

immune and chemically triggered oxidative stress modifies translational fidelity. Nature **462,** 522-526

8. Marshall, L., Kenneth, N. S., and White, R. J. (2008) Elevated $tRNAi^{Met}$ synthesis can drive cell proliferation and oncogenic transformation. Cell **133,** 78-89

9. Park, S. G., Choi, E. C., and Kim, S. (2010) Aminoacyl-tRNA synthetase-interacting multifunctional proteins (AIMPs): a triad for cellular homeostasis. IUBMB Life **62,** 296-302

10. Han, J. M., Lee, M. J., Park, S. G., Lee, S. H., Razin, E., Choi, E. C., and Kim, S. (2006) Hierarchical network between the components of the multi-tRNA synthetase complex: implications for complex formation. J. Biol. Chem. **281,** 38663-38667

11. Park, B. J., Kang, J. W., Lee, S. W., Choi, S. J., Shin, Y. K., Ahn, Y. H., Choi, Y. H., Choi, D., Lee, K. S., and Kim, S. (2005) The haploinsufficient tumor suppressor p18 upregulates p53 via interactions with ATM/ATR. Cell **120,** 209-221

12. Quevillon, S., Robinson, J. C., Berthonneau, E., Siatecka, M., and Mirande, M. (1999) Macromolecular assemblage of aminoacyl-tRNA synthetases: identification of protein-protein interactions and characterization of a core protein. J. Mol. Biol. **285,** 183-195

13. Rho, S. B., Kim, M. J., Lee, J. S., Seol, W., Motegi, H., Kim, S., and Shiba, K. (1999) Genetic dissection of protein-protein interactions in multi-tRNA synthetase complex. Proc. Natl. Acad. Sci. U.S.A. **96,** 4488-4493

14. Kim, K. J., Park, M. C., Choi, S. J., Oh, Y. S., Choi, E. C., Cho, H. J., Kim, M. H., Kim, S. H., Kim, D. W., Kim, S., and Kang, B. S. (2008) Determination of three-dimensional structure and residues of the novel tumor suppressor AIMP3/p18 required for the interaction with ATM. J. Biol. Chem. **283,** 14032-14040

15. Park, B. J., Oh, Y. S., Park, S. Y., Choi, S. J., Rudolph, C., Schlegelberger, B., and Kim, S. (2006) AIMP3 haploinsufficiency disrupts oncogene-induced p53 activation and genomic stability. Cancer Res. **66,** 6913-6918

16. Kaminska, M., Deniziak, M., Kerjan, P., Barciszewski, J., and Mirande, M. (2000) A recurrent general RNA binding domain appended to plant methionyl-tRNA synthetase acts as a cis-acting cofactor for aminoacylation. EMBO J. **19,** 6908-6917

17. Guo, M., Yang, X. L., and Schimmel, P. (2010) New functions of aminoacyl-tRNA synthetases beyond translation. Nat. Rev. Mol. Cell Biol. **11,** 668-674

18. Wek, R. C., Jiang, H. Y., and Anthony, T. G. (2006) Coping with stress: eIF2 kinases and translational control. Biochem. Soc. Trans. **34,** 7-11

19. Shyu, Y. J., Suarez, C. D., and Hu, C. D. (2008) Visualization of ternary complexes in living cells by using a BiFC-based FRET assay. Nat. Protoc. **3,** 1693-1702

20. Srivastava, S. P., Kumar, K. U., and Kaufman, R. J. (1998) Phosphorylation of eukaryotic translation initiation factor 2 mediates apoptosis in response to activation of the double-stranded RNA-dependent protein kinase. J. Biol. Chem. **273,** 2416-2423

21. Raven, J. F., and Koromilas, A. E. (2008) PERK and PKR: old kinases learn new

tricks. Cell Cycle **7,** 1146-1150

22. Deng, J., Harding, H. P., Raught, B., Gingras, A. C., Berlanga, J. J., Scheuner, D., Kaufman, R. J., Ron, D., and Sonenberg, N. (2002) Activation of GCN2 in UV-irradiated cells inhibits translation. Curr. Biol. **12,** 1279-1286

23. Berlanga, J. J., Santoyo, J., and De Haro, C. (1999) Characterization of a mammalian homolog of the GCN2 eukaryotic initiation factor 2alpha kinase. Eur. J. Biochem. **265,** 754-762

24. Dong, J., Qiu, H., Garcia-Barrio, M., Anderson, J., and Hinnebusch, A. G. (2000) Uncharged tRNA activates GCN2 by displacing the protein kinase moiety from a bipartite tRNA-binding domain. Mol. Cell **6,** 269-279

25. Wek, S. A., Zhu, S., and Wek, R. C. (1995) The histidyl-tRNA synthetase-related sequence in the eIF-2 alpha protein kinase GCN2 interacts with tRNA and is required for activation in response to starvation for different amino acids. Mol. Cell Biol. **15,** 4497-4506

26. Jiang, H. Y., and Wek, R. C. (2005) GCN2 phosphorylation of eIF2alpha activates NF-kappaB in response to UV irradiation. Biochem. J. **385,** 371-380

27. He, R., Zu, L. D., Yao, P., Chen, X., and Wang, E. D. (2009) Two non-redundant fragments in the N-terminal peptide of human cytosolic methionyl-tRNA synthetase were indispensable for the multi-synthetase complex incorporation and enzyme activity. Biochim. Biophys. Acta. **1794,** 347-354

28. Nakanishi, K., Ogiso, Y., Nakama, T., Fukai, S., and Nureki, O. (2005) Structural basis for anticodon recognition by methionyl-tRNA synthetase. Nat. Struct. Mol. Biol. **12,** 931-932

29. Ghosh, A., and Vishveshwara, S. (2007) A study of communication pathways in methionyl- tRNA synthetase by molecular dynamics simulations and structure network analysis. Proc. Natl. Acad. Sci. U.S.A. **104,** 15711-15716

30. Oh, Y. S., Kim, D. G., Kim, G., Choi, E. C., Kennedy, B. K., Suh, Y., Park, B. J., and Kim, S. (2010) Downregulation of laminA by tumor suppressor AIMP3/p18 leads to a progeroid phenotype in mice. Aging Cell **9,** 810-822

31. Arif, A., Jia, J., Mukhopadhyay, R., Willard, B., Kinter, M., and Fox, P. L. (2009) Two-site phosphorylation of EPRS coordinates multimodal regulation of noncanonical translational control activity. Mol. Cell **35,** 164-180

32. Lee, Y. N., Nechushtan, H., Figov, N., and Razin, E. (2004) The function of lysyl-tRNA synthetase and Ap4A as signaling regulators of MITF activity in FcepsilonRI-activated mast cells. Immunity **20,** 145-151

33. Han, J. M., Park, B. J., Park, S. G., Oh, Y. S., Choi, S. J., Lee, S. W., Hwang, S. K., Chang, S. H., Cho, M. H., and Kim, S. (2008) AIMP2/p38, the scaffold for the multi-tRNA synthetase complex, responds to genotoxic stresses via p53. Proc. Natl. Acad. Sci. U.S.A. **105,** 11206-11211

34. Grallert, B., and Boye, E. (2007) The Gcn2 kinase as a cell cycle regulator. Cell

Cycle **6,** 2768-2772

35. Schaefer, E. M., and Guimond, S. (1998) Detection of protein tyrosine kinase activity using a high-capacity streptavidin-coated membrane and optimized biotinylated peptide substrates. Anal. Biochem. **261,** 100-112

36. Kohrer, C., and Rajbhandary, U. L. (2008) The many applications of acid urea polyacrylamide gel electrophoresis to studies of tRNAs and aminoacyl-tRNA synthetases. Methods **44,** 129-138

PART II.

AIMP3/p18 regulates translational initiation by the delivery of methionine through the formation of initiation ternary complex

Keywords : AIMP3, MRS, translation initiation, methionine, initiator tRNA, eukaryotic initiation factor 2 subunit gamma (eIF2γ)

ABSTRACT

Aminoacyl-tRNA synthetases (ARSs) attach specific amino acids to their cognate tRNAs in protein synthesis process. In higher eukaryote, nine ARSs form multi-synthetase complex (MSC) with three cofactors designated ARS-interacting multifunctional proteins (AIMPs). Methionyl-tRNA synthetase (MRS), which attaches methionine to initiator tRNA ($tRNA_i^{Met}$), associates with AIMP3. However the role of AIMP3 in translation as a component of MSC and the meaning of its interaction with MRS are still unclear. Herein, I showed that AIMP3 specifically binds charged $tRNA_i^{Met}$ (Met-$tRNA_i^{Met}$). In addition, AIMP3 discriminated Met-$tRNA_i^{Met}$ from methionine-charged elongator tRNA based on filter-binding assay. AIMP3 and MRS bound with gamma subunit of eukaryotic initiation factor 2 (eIF2γ), which is in charge of binding with Met-$tRNA_i^{Met}$ for the delivery of Met-$tRNA_i^{Met}$ to ribosome. AIMP3 recruited active eIF2γ (eukaryotic initiation factor 2 gamma subunit) to the MRS-AIMP3 complex, facilitating precise and efficient transfer of Met-$tRNA_i^{Met}$ to eIF2γ. The knockdown of AIMP3 reduced protein synthesis and the level of Met-$tRNA_i^{Met}$ bound to eIF2 complex. This study suggests the novel function of AIMP3 as a critical mediator of Met-$tRNA_i^{Met}$ transfer from MRS to eIF2 complex for the accurate and efficient translation initiation.

INTRODUCTION

Aminoacyl-tRNA synthetases (ARSs), which ligate amino acids to their cognate tRNAs, form a multisynthetase complex (MSC) in higher eukaryotes (1). This complex consists of 9 ARSs and 3 nonenzymatic cofactors called ARS-interacting multifunctional proteins (AIMPs), namely, AIMP1/p43, AIMP2/p38, and AIMP3/p18 (2). AIMPs are related with scaffolding the MSC structure and controlling the stability of neighboring ARSs (3). Furthermore, AIMPs dissociate from MSC in response to various stimuli and are involved in diverse biological functions and signaling pathways, such as immune responses, angiogenesis, wound healing, glucose homeostasis, cell proliferation, and apoptosis (4-11). Among them, AIMP3 is known to be a potent tumor suppressor via activation of p53 under UV damage or oncogenic stress (12, 13), and overexpression of AIMP3 can drive cellular senescence via degradation of mature lamin A (14).

While my understanding of the functions of AIMPs outside MSC has advanced considerably, their roles in the MSC as translation components remain unclear. Arc1p, a yeast orthologue of human AIMP1/p43, is known to increase the aminoacylation activities of methionyl-tRNA synthetase (MRS) and glutamyl-tRNA synthetase by recruiting tRNAs (15, 16). AIMP1 also binds to tRNA and enhances the aminoacylation activity of arginyl-tRNA synthetase

(RRS) (17). AIMP3 has sequence similarity to valyl-tRNA synthetase and is also known as eukaryotic elongation factor 1 epsilon 1 (eEF1ε1) based on sequence similarity to eEFs (18). These results imply that AIMPs can play an important role in the translation process as members of MSC, although little is known about their functions in protein synthesis.

AIMP3 strongly associates with MRS in the MSC, and knockdown of AIMP3 affects the stability of MRS protein (3). Recently, the importance of MRS in global translational regulation was suggested (19). Under UV irradiation, MRS was phosphorylated by GCN2, and this modification reduced the catalytic activity of MRS, resulting in decreased levels of charged initiator tRNA (Met-$tRNA_i^{Met}$). For translation initiation, Met-$tRNA_i^{Met}$ should bind to eukaryotic initiation factor 2 (eIF2) in a GTP-dependent manner to form the ternary complex, eIF2·GTP·Met-$tRNA_i^{Met}$, which delivers Met-$tRNA_i^{Met}$ to the 40S ribosomal subunit (20). That is the reason why MRS phosphorylation and insufficient ternary complex formation can reduce global protein synthesis.

Because AIMP3 specifically binds to MRS in the MSC and AIMP3 has sequence similarity to eEFs, I hypothesized that AIMP3 may have a function in translation regarding MRS activation or Met-$tRNA_i^{Met}$ delivery to other translation factors. Here, it is reported that AIMP3 interacts with Met-$tRNA_i^{Met}$ and the eIF2 complex and plays an important role in connecting aminoacylation

to translation. These results suggest that AIMP3 may be a critical mediator of the accurate and efficient delivery of the Met-$tRNA_i^{Met}$ to eIF2 and a regulator of global translation initiation.

RESULTS

AIMP3 specifically binds to Met-tRNA$_i^{Met}$

Arc1p, as a cofactor of MRS and ERS, enhances the aminoacylation activity through the tRNA attraction in yeast (15, 16). To test whether AIMP3 can effect as like Arc1p, I examined the binding affinity of AIMP3 to free or charged tRNA$_i^{Met}$ using a filter binding assay. The MRS and eIF2 gamma subunit (eIF2γ) were used as controls for the binding with tRNA$_i^{Met}$ and Met-tRNA$_i^{Met}$, respectively. In this assay, AIMP3 did not show interaction with *in vitro* transcribed radioactive tRNA$_i^{Met}$ (Figure II-1A). In contrast, AIMP3 revealed explicit interaction to Met-tRNA$_i^{Met}$ in a dose-dependent manner (Figures II-1B and C). Because AIMP3 only bound to Met-tRNA$_i^{Met}$, I hypothesized that AIMP3 might recognize methionine attached to the acceptor stem of tRNA$_i^{Met}$. To test this, the interaction between AIMP3 and radioactive methionine was analyzed and AIMP3 has binding affinity to methionine as expected (Figure II-1D). Next, I prepared Met-tRNA$_i^{Met}$ and Met-tRNA$_e^{Met}$ to examine the difference between tRNA^{Met} isoforms with regard to recognition by AIMP3, and I also charged these tRNAs with nonnatural amino acid acetylate lysine (acK) to compare its binding affinity to AIMP3 with that of methionine. Interestingly, the association between AIMP3 and Met-tRNA$_i^{Met}$ was detected more obvious

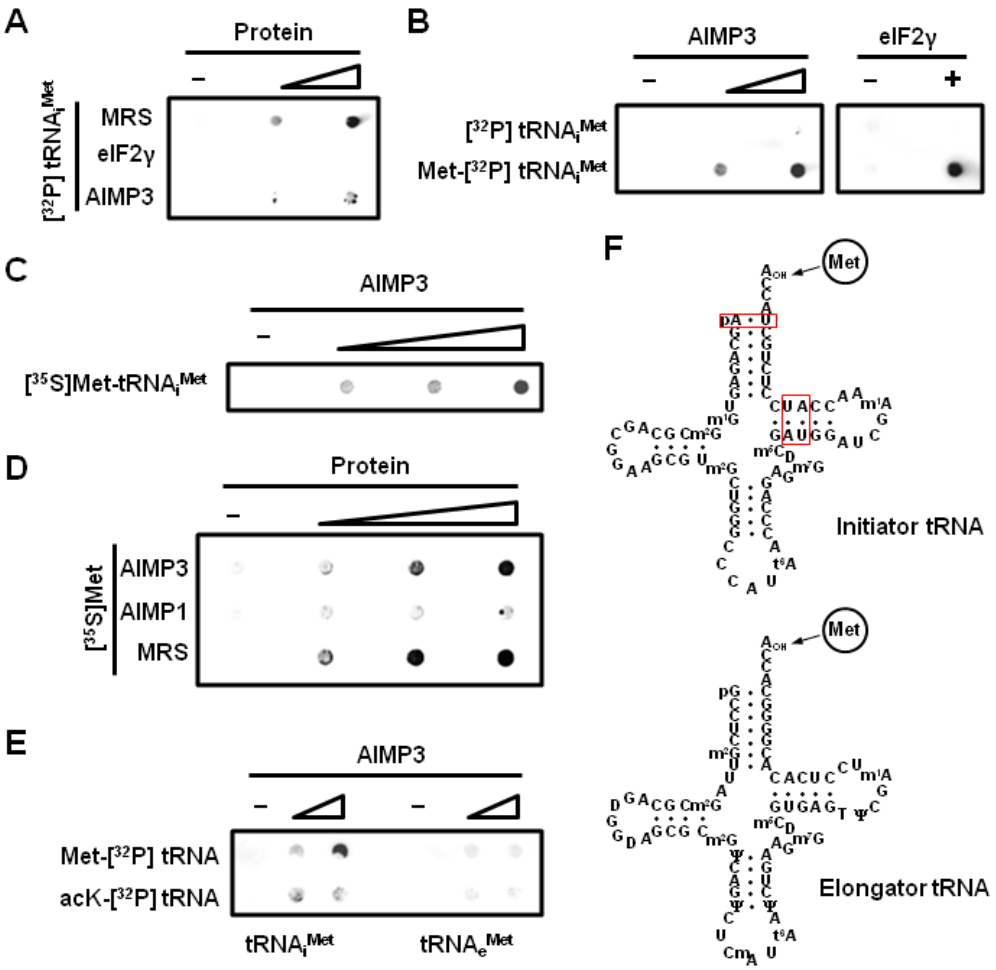

Figure II-1. Specific interaction between AIMP3 and Met-tRNA$_i^{Met}$. (A) Radioactively labeled free [^{32}P]tRNA$_i^{Met}$ was incubated with His-tagged MRS, eIF2γ, and AIMP3. Signals from tRNA bound to proteins were detected by autoradiography. **(B)** Unacylated tRNA$_i^{Met}$ and charged Met-[^{32}P]tRNA$_i^{Met}$ were subjected to a filter-binding assay with AIMP3 and eIF2γ. **(C)** tRNA$_i^{Met}$ was charged with [^{35}S]methionine and used for the binding assay to investigate the interaction between Met-tRNA$_i^{Met}$ and AIMP3. **(D)** Interaction between AIMP3 and methionine was determined by the filter-binding assay. MRS and AIMP1 were used as the positive and negative controls,

respectively. **(E)** Radioactively labeled $tRNA_i^{Met}$ and $tRNA_e^{Met}$ were charged with mehionine and acetylated lysine (acK) using MRS and dFx, respectively, and their interaction with AIMP3 was analyzed by filter binding assay. AcK, a nonnatural amino acid, was used as a substitute for comparison with methionine. **(F)** The secondary structure of human $tRNA_i^{Met}$ and $tRNA_e^{Met}$. Boxed nucleotides indicate discriminating basepairs of $tRNA_i^{Met}$, whose mutations make $tRNA_i^{Met}$ work as $tRNA_e^{Met}$ (28). Methionine is attached to 3' OH group via an ester linkage by MRS.

than any other types of tRNAs tested (Figure II-1E). All together, these results imply that AIMP3 has binding preference to $tRNA_i^{Met}$ over $tRNA_e^{Met}$ only when they are charged with methionine. Although AIMP3 knockdown affected the stability of MRS, resulting in reduced aminoacylation activity of MRS in *AIMP3*$^{+/-}$ mouse embryonic fibroblast (MEF) cells, AIMP3 showed no direct effect on the catalytic reaction *in vitro* (Figure II-2A and B).

MRS and AIMP3 interact with eIF2γ

Because AIMP3 did not affect the catalytic activity of MRS, AIMP3 was supposed to mediate the Met-$tRNA_i^{Met}$ delivery to downstream proteins. Considering translation steps, Met-$tRNA_i^{Met}$ should be transferred to eIF2 complex for the formation of the initiation ternary complex, therefore, I analyzed the interaction among MRS, AIMP3 and eIF2α, β and γ subunits. The GST-pull down assays revealed that MRS and AIMP3 commonly interacted with eIF2γ among the eIF2 subunits (Figures II-3A and B), which is in charge of binding with Met-$tRNA_i^{Met}$ as well as GTP (21). MRS and eIF2γ were pulled down together by association with AIMP3 (Figure II-3C), suggesting that this tripartite interaction is not mutually exclusive. I identified the binding domains of MRS and AIMP3, assigned to interact with eIF2γ, using deletion mutants, and confirmed that MRS and AIMP3 used different domains for each

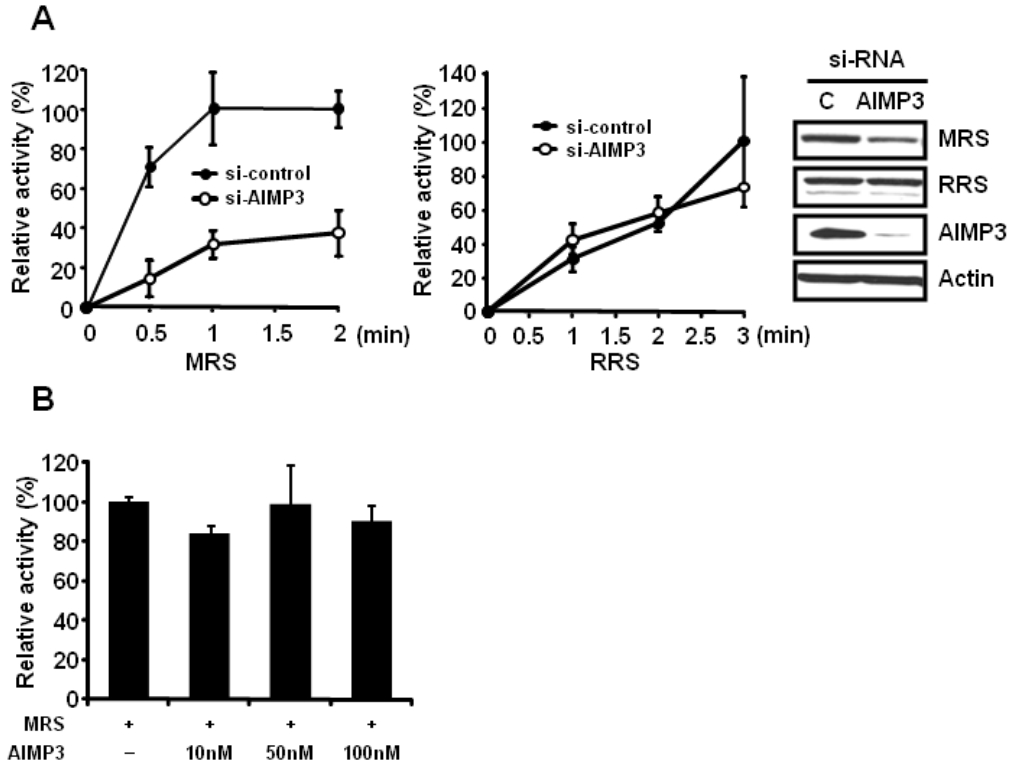

Figure II-2. Effect of AIMP3 on the aminoacylation activity of MRS. (A) HeLa cells transfected with siRNA were lysed and the catalytic activities for MRS and RRS in the cell lysate were analyzed by aminoacylation assay. Data are presented as mean +/− SD (n=3). Proteins levels in the cell lysate were also presented by immunoblotting. **(B)** Relative activity of purified MRS (50 nM) was determined in absence and presence of various concentration of AIMP3 (10, 50, 100 nM). The experiments were repeated three times.

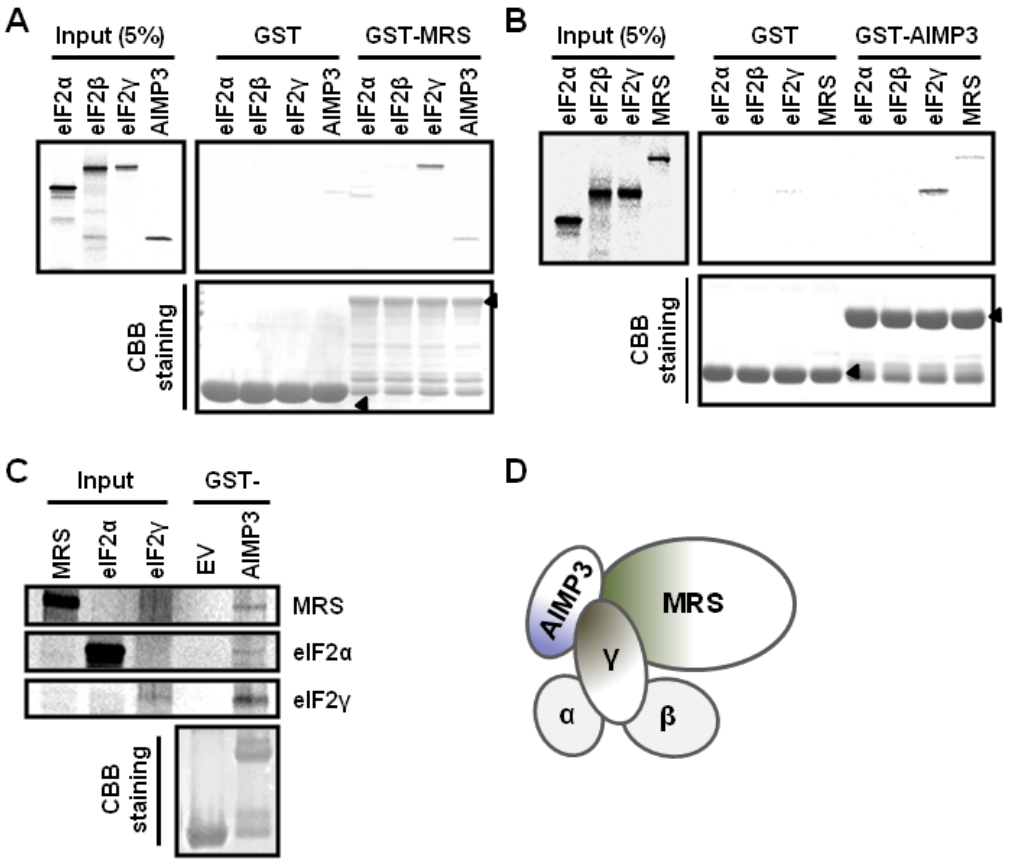

Figure II-3. Interaction of AIMP3 and MRS with eIF2γ. (A and B) Radioactively labeled eIF2 subunits, eIF2α, eIF2β, and eIF2γ, were incubated with GST-MRS or GST-AIMP3. The bound eIF2 subunits were detected by autoradiography. Each protein, stained with Coomassie Brilliant Blue (CBB), is indicated by an arrow. **(C)** Radioactively labeled eIF2α, eIF2γ, and MRS were mixed with GST-AIMP3. Bound proteins were detected by autoradiography. eIF2α, a binding partner of eIF2γ, was also included to investigate the possibility of eIF2-complex association with the MRS-AIMP3 complex. **(D)** Interactions between MRS, AIMP3, and the eIF2 subunits (α, β, and γ) are schematically presented based on domain mapping (Figure II-4). The N-termini of these proteins are indicated by dense coloration.

binding partner to perform non-competitive association with eIF2γ (Figure II-3D and Figure II-4). This domain mapping suggests that GST homology domains of MRS and AIMP3 are important for binding with eIF2γ and GTP binding domain of eIF2γ is crucial for binding to MRS and AIMP3.

AIMP3 recruits active eIF2γ and facilitate its interaction to MRS

Since the binding domains of each protein were not overlapped, the interactions among MRS, AIMP3 and eIF2γ may be regulated by one protein working as an adapter. To examine whether AIMP3 can mediate the interaction between MRS and eIF2γ, I knocked down AIMP3 in HeLa cells using RNAi and analyzed the change in interaction by immunoprecipitation (IP) assay. As expected, interaction of eIF2γ with MRS was decreased in AIMP3 knockdown cells (Figure II-5A). This result suggests that interaction of MRS and eIF2γ is dependent on the existence of AIMP3. To determine the possibility that AIMP3 can recruit active eIF2γ, I substituted Asn to Asp at 190 residue in the NKXD consensus sequence of eIF2γ, which is known to be an important site for GTP binding (22). The N190D mutant mimics inactive eIF2γ, and it revealed reduced binding to AIMP3 in comparison with wild type (WT) eIF2γ in the IP assay (Figure II-5B). These results elucidated that AIMP3 was critical for the binding between MRS and eIF2γ, and as well as for the recruitment of active eIF2γ to

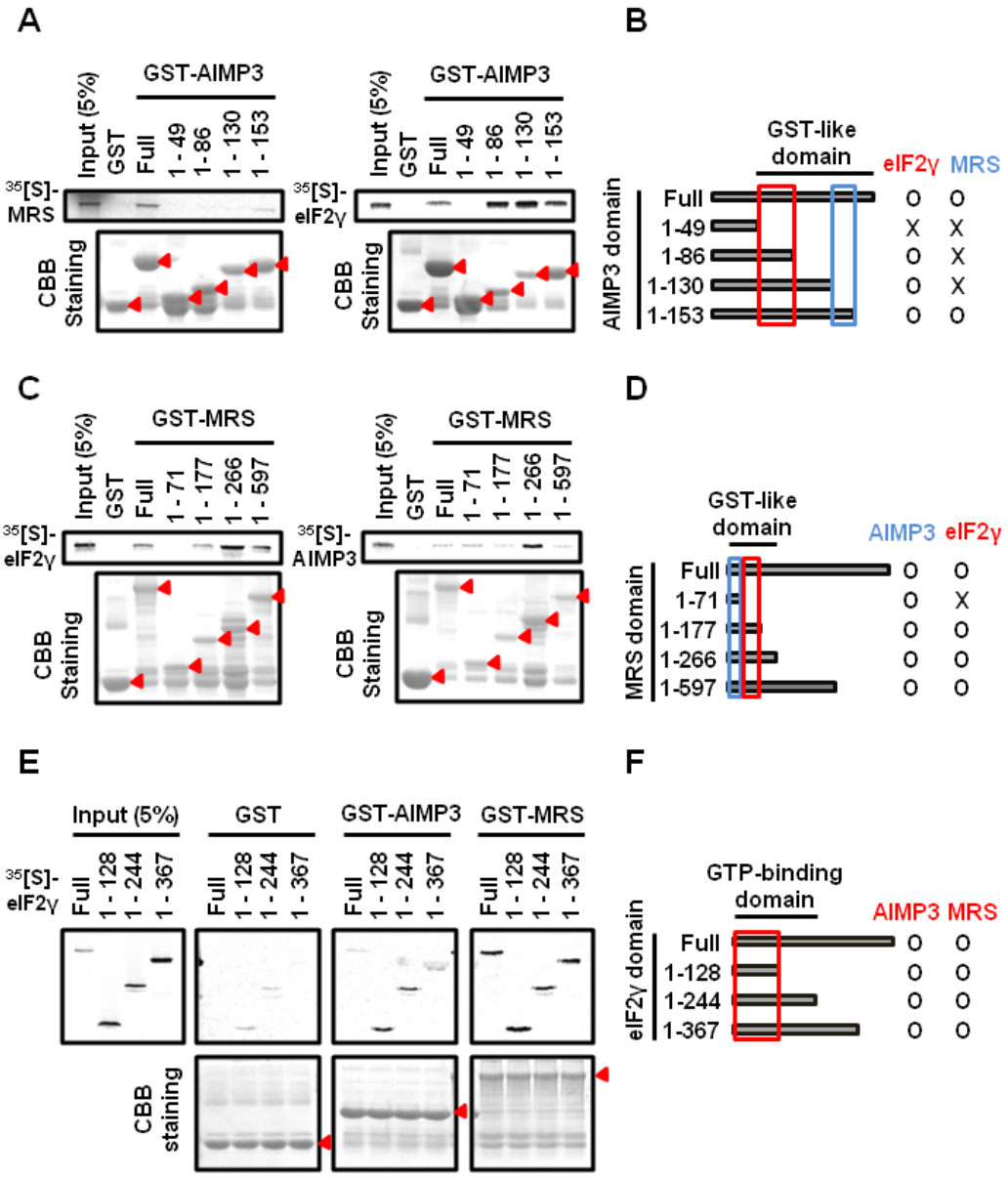

Figure II-4. Domain mapping for the interaction among MRS, AIMP3 and eIF2γ. **(A)** Radioactively synthesized MRS or eIF2γ was incubated with deletion domains of immobilized GST-AIMP3 and then exposed for autoradiography. **(C)** The binding of radiolabeled eIF2γ or AIMP3 to GST-MRS deletion mutants was analyzed using pull

down assay. **(E)** GST-AIMP3 and GST-MRS were incubated with radioactively labeled eIF2γ deletion mutants. Bound proteins were detected by autoradiography. Each protein, stained with CBB, is indicated by an arrow.

Schematic diagram for each binding motif identified was also represented in each panel. **(B)** AIMP3 domains for the binding with eIF2γ and MRS are indicated as red and blue boxes, respectively. **(D)** MRS domains which interact with eIF2γ and AIMP3 are indicated as red and blue boxes, respectively. **(F)** The domain of eIF2γ which in charge with AIMP3 and MRS binding is shown in red box.

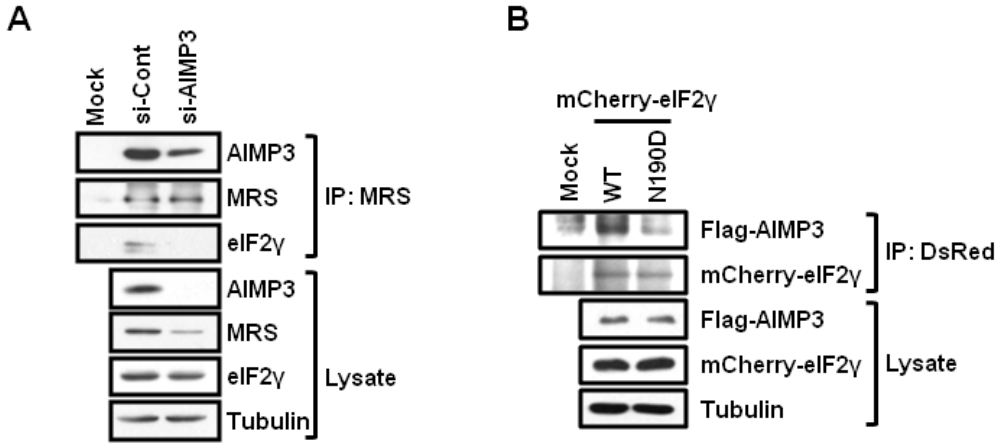

Figure II-5. The effect of AIMP3 on the interaction between MRS and eIF2γ. (A) HeLa cells were transfected with si-control and si-AIMP3. MRS was immunoprecipitated, and the bound proteins were analyzed using western blotting. As MRS levels in the cells treated with si-AIMP3 were reduced, minimum amounts of anti-MRS antibody (0.5 μg/500 μl lysate) were used for the IP assays to equalize the amounts of captured MRS between the samples. **(B)** 293T cells were transfected with mCherry-tagged eIF2γ (WT or N190D mutant) and Flag-AIMP3 simultaneously, and the mCherry-eIF2γ proteins were immunoprecipitated using anti-DsRed antibody for the analysis of bound Flag-AIMP3. WCL and bound proteins were determined by immunoblotting with specific antibodies.

MRS-AIMP3 complex.

AIMP3 is important for the ternary complex formation

Because AIMP3 interacted with Met-$tRNA_i^{Met}$ as well as eIF2γ specifically, I examined whether AIMP3 could play a role in the formation of initiation ternary complex via delivery of Met-$tRNA_i^{Met}$. HeLa cells were transfected with specific siRNAs for knockdown of MRS, AIMP3, eIF2α and eIF2γ, and ternary complex was immunoprecipitated with eIF2β-specific antibody. The amount of $tRNA_i^{Met}$ bound to eIF2 complex was analyzed, revealing that downregulation of AIMP3 decreased $tRNA_i^{Met}$ in eIF2 complex to the same level as seen in eIF2γ knockdown (Figure II-6A). The effect of MRS or eIF2α knockdown on the amount of $tRNA_i^{Met}$ was not so critical as much as AIMP3. Next I carried out a gel filtration assay to confirm the effect of AIMP3 knockdown on the colocalization of eIF2 complex with ribosome. As expected, reduced levels of AIMP3 decreased the amounts of eIF2 subunits in the ribosomal fraction in comparison with MRS-knockdown (Figure II-6B), suggesting that levels of AIMP3 affected ternary complex formation, which should be detected in the ribosome fraction (23). All together, these results indicated that AIMP3 played a crucial role in ternary complex formation that was linked to protein synthesis. To confirm the global effect of AIMP3 on global translation, I calculated protein

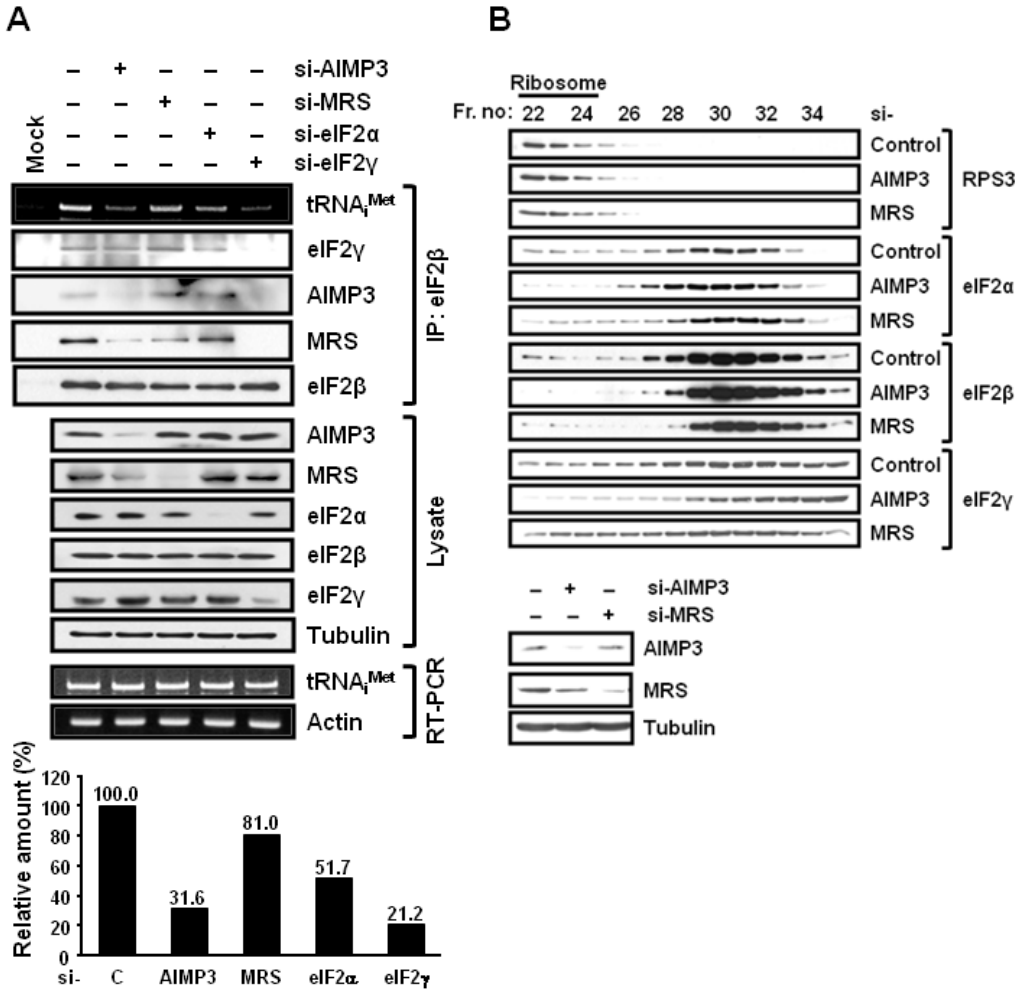

Figure II-6. The effect of AIMP3 on ternary complex formation. (A) Ternary complex was immunoprecipitated with anti-eIF2β antibody from the siRNA-transfected HeLa cells. The bound RNA was purified using Trizol, and the amounts of bound tRNA$_i^{Met}$ were analyzed using RT-PCR. Actin was used as a loading control. The immunoprecipitated proteins and WCL were analyzed by immunoblotting. **(B)** Five mg of HeLa cell lysates transfected with siRNA were subjected to gel filtration assay and fractionized by protein size. RPS3 was used as a marker of ribosomal fraction. Ribosome was fractionized in the fraction (Fr.) #22~24.

synthesis rate in *AIMP3* MEF and HeLa cells using a methionine incorporation assay. *AIMP3*$^{+/-}$ MEF cells showed about 40% reduction of translation as compared with *AIMP3*$^{+/+}$ MEF cells (Figure II-7A), and similar results were obtained with si-AIMP3 transfected HeLa cells (Figure II-7B). Global translation was also reduced approximately 20% by the knockdown of MRS; however, the knockdown effect of AIMP3 was more efficient on protein synthesis. These results demonstrated the importance of Met-tRNA$_i^{Met}$ delivery to eIF2 via AIMP3 in the global translation, even when Met-tRNA$_i^{Met}$ seemed to be produced enough not to delay ternary complex formation.

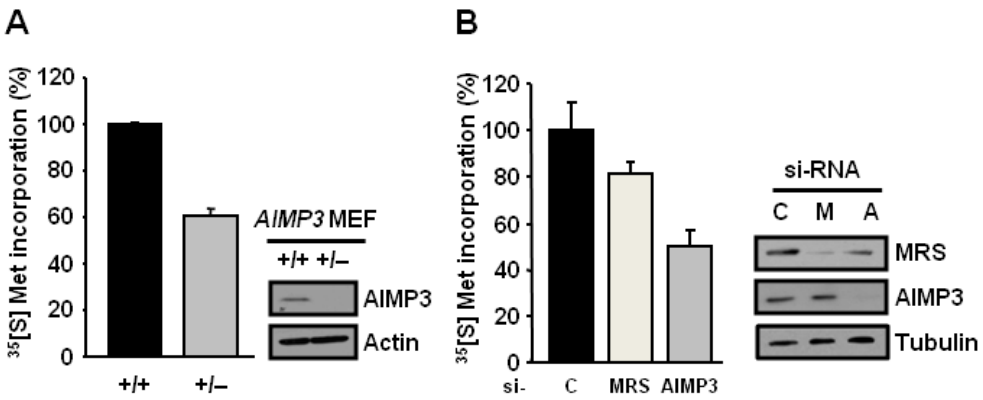

Figure II-7. The effect of AIMP3 on global translation. Protein synthesis in the AIMP3$^{+/+}$ and AIMP3$^{+/-}$ MEFs (**A**) and siRNA-transfected HeLa cells (**B**) was analyzed using a methionine incorporation assay. Mean ± S.D. of triplicate experiments are shown. The differences between the samples were significant ($P < 0.05$, one-way ANOVA), Si-C, si-control; si-M, si-MRS; si-A, si-AIMP3. The decreased level of AIMP3 affected protein synthesis rate.

DISCUSSION

Recently, another group reported a model that explains how the ternary complex binds the 40S ribosomal subunit by identifying the binding motifs of eIF2γ and 40S ribosome (24). However, it is unclear how Met-$tRNA_i^{Met}$ moves to eIF2γ from MRS in the early stage of translation initiation. I demonstrated here that AIMP3, a binding partner of MRS in the MSC, worked as a mediator of Met-$tRNA_i^{Met}$ delivery from MRS to eIF2 (Figure II-8). It is interesting that AIMP3 exhibits high affinity for Met-$tRNA_i^{Met}$ but not Met-$tRNA_e^{Met}$, and it affected ternary complex formation, which is critical for translation initiation.

MRS acylates $tRNA_i^{Met}$ and $tRNA_e^{Met}$, and among the acylated tRNAs, only Met-$tRNA_i^{Met}$ was recognized by AIMP3, suggesting that AIMP3 is probably involved in the translation initiation but not elongation step. The GTP-bound form of eIF2γ can also interact with Met-$tRNA_i^{Met}$ through the recognition of methionine moiety (21). This suggests to us that tRNA sequences and methionine are important for binding to AIMP3 and eIF2γ. While $tRNA_i^{Met}$ and $tRNA_e^{Met}$ share the same anti-codon sequences, there are several differences between them (Figure II-1F). One of the most distinctive features of $tRNA_i^{Met}$ relates to the acceptor stem, where the discriminating base pair is located. $tRNA_i^{Met}$ has an A1:U72 base pair in its acceptor stem, whereas $tRNA_e^{Met}$ has an

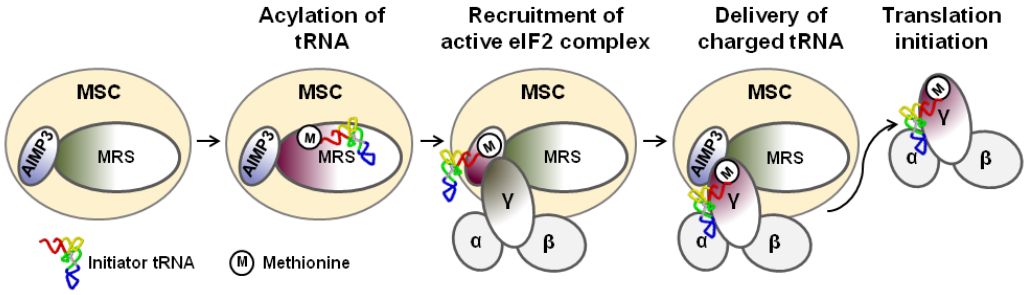

Figure II-8. Schematic representation of tRNA transfer mediated by AIMP3. In general, AIMP3 interacts with MRS in the MSC. For translation initiation, MRS catalyzes attachment of methionine to $tRNA_i^{Met}$. Met-$tRNA_i^{Met}$ is released from MRS and binds to AIMP3. AIMP3 recruits active eIF2γ and transfers Met-$tRNA_i^{Met}$ to eIF2γ for ternary complex formation. In each step, Met-$tRNA_i^{Met}$-interacting protein is shown in violet.

G1:C72 base pair (21, 25). Because of this difference, eIF2γ can discriminate Met-$tRNA_i^{Met}$ from Met-$tRNA_e^{Met}$. AIMP3 and eIF2γ may recognize Met-$tRNA_i^{Met}$ in a same way, although more study is required to fully understand the Met-$tRNA_i^{Met}$ delivery mechanism.

It seems that MRS also interacts with eIF2γ. Direct delivery of Met-$tRNA_i^{Met}$ from MRS to eIF2γ without the involvement of AIMP3 is probably the easier way. However, AIMP3 involvement can inhibit diffusion of Met-$tRNA_i^{Met}$ by recruiting active eIF2γ to the MRS-AIMP3 complex, thereby increases the efficiency and accuracy of ternary complex formation. AIMP3 involvement in Met-$tRNA_i^{Met}$ transfer may be meaningful, considering the complicated regulatory mechanism of translation in higher eukaryotes. Generally, translation is regulated by phosphorylation of eIF2α. This phosphorylation prevents formation of the ternary complex and inhibits further rounds of translation initiation. In addition, a recent study has suggested another mechanism of translation control under UV stress (19). MRS phosphorylation occurred simultaneously with eIF2α phosphorylation and inhibited translation by reducing Met-$tRNA_i^{Met}$ production. The MRS phosphorylation site is critical for tRNA binding; however, this residue is not conserved in lower eukaryotes, such as yeast. AIMP3 only exists in higher eukaryotes, but its various functions are essential for the maintenance of life in higher eukaryotes (12-14). These studies

suggest that translational regulation mediated by MRS and AIMP3 may be an adaptation by higher eukaryotes, which developed more accurate and multi-step translational regulation during evolution. In the present study, I elucidated the role of AIMP3 as a subunit of MSC. Furthermore, I determined that AIMP3 can capture the charged initiator tRNA and deliver it to eIF2 by recruiting active eIF2γ and that AIMP3 enables precise and efficient formation of the ternary complex and affects global translation.

MATERIALS AND METHODS

Cell culture and transfection

293T, HeLa and AIMP3 MEF cells were maintained in Dulbecco's modified Eagle's medium (DMEM, Hyclone) supplemented with 10% fetal bovine serum and 50 μg/ml penicillin/streptomycin in 5% CO_2 at 37 ℃. Plasmids and siRNAs were transfected using Fugene HD (Roche) and Lipofectamine 2000 (Invitrogen), respectively, according to the manufacturer's instruction.

Antibodies

Antibodies for the detection of tubulin (mouse, T6074, Sigma), Flag (mouse, F3156, Sigma), GFP (mouse, sc-9996, Santa Cruz), DsRed (rabbit, 632496, Clontech), eIF2α (rabbit, sc-11386, Santa Cruz), eIF2β (mouse, sc-9978, Santa Cruz), eIF2γ (mouse, H00001968-M01, Abnova), and Ribosomal protein S3 (RPS3, rabbit, #2579S, Cell Signaling) were purchased and used for western blot and immunoprecipitation assays. Antibodies for MRS, RRS and AIMP3 were previously described (17, 19).

Protein purification and aminoacylation assay

His-MRS, His-AIMP3 and His-eIF2γ were obtained from *E. coli* Rosetta(DE3)

by IPTG induction and purified as described, with modification of imidazole concentration (50 mM) for AIMP3 at the final washing step. His-eIF2γ was purified under denaturing method with 8 M urea buffer. Eluted proteins were refolded with dialysis buffer by gradually decreasing concentration of urea. MRS aminoacylation reaction with recombinant human MRS was performed as described (19). For the detection of MRS activity in cell lysate, HeLa cells were lysed with hypotonic buffer (25 mM Tris-HCl pH 7.4, 10 mM NaCl, 0.5 mM EDTA and 10 mM Sucrose) containing protease inhibitor cocktail (Calbiochem), and 20 μg of lysate proteins were used for the aminoacylation assay.

Preparation of charged $tRNA^{Met}$

[α-^{32}P]UTP (3000 Ci/mmol, Izotop)-labeled $tRNA_i^{Met}$ or elongator $tRNA_e^{Met}$ was synthesized by *in vitro* transcription with T7 RNA polymerase, using a tRNA expression vector as the template (19). To produce charged $tRNA^{Met}$, an aminoacylation reaction was performed in reaction buffer containing 30 mM HEPES (pH 7.4), 100 mM potassium acetate, 10 mM magnesium acetate, 2 mM ATP, 2 mM methionine, 5 μl [α-^{32}P]$tRNA_i^{Met}$, and recombinant human MRS. Charged tRNA was purified using phenol/chloroform extraction in the presence of sodium acetate (pH 5.2). [α-^{32}P]tRNA charged with acetylated lysine (acK) was prepared by dFx (dinitro-flexizyme, a ribozyme-based tRNA-acylating

catalyst) as described previously (26). For the labeling of Met-$tRNA_i^{Met}$ with [^{35}S]methionine, radioisotope-free $tRNA_i^{Met}$ (500 μg/ml) was synthesized and incubated in reaction buffer with the addition of 20 μM methionine and 25 μCi [^{35}S]methionine (1000 Ci/mmol, Izotop) and then purified as described earlier.

Filter-binding assay (dot blot assay)

Synthesized tRNA or charged tRNA (150,000 cpm/μl) was incubated with proteins in binding buffer (20 mM Tris-HCl pH 7.4, 75 mM KCl, 10 mM $MgCl_2$, and 5% glycerol) at 30 ℃ for 30 min. The reaction mixtures were filtered through pre-equilibrated nitrocellulose membranes (GE Healthcare) using a 96-well minifold filtration apparatus (Bio-Dot apparatus, Bio-Rad). Dried membranes were exposed, and signals were detected by autoradiography.

GST pull-down assay

GST fusion proteins were expressed and induced in *Escherichia coli* BL21(DE3) strain, and then the harvested bacteria were lysed by sonication. The lysates were incubated with glutathione sepharese 4B (GE Healthcare) in lysis buffer (PBS containing 0.5% Triton X-100, 1 mM EDTA, 1 mM dithiothreitol, and protease inhibitor) at 4 ℃ for 6 h. Radioactively synthesized proteins were incubated with immobilized GST fusion protein in lysis buffer at 4 ℃ for 4 h. The beads

were washed 3 times with lysis buffer and added in SDS sample buffer. Bound proteins were separated by SDS-PAGE and detected by autoradiography.

Detection of $tRNA_i^{Met}$ from the ternary complex

For the detection of bound tRNA from the ternary complex, HeLa cells were lysed with buffer A (20 mM Tris-HCl pH 7.5, 100 mM KCl, 5 mM $MgCl_2$, 100 μM EDTA, 7 mM β-mercaptoethanol, 5 mM NaF, 1 mM PMSF, and 1 mM RNase inhibitor) and ternary complex was immunoprecipitated using an eIF2β-specific antibody (27). After washing with buffer A, the bound RNA was purified using Trizol (Invitrogen), and the extracted RNAs were subjected to reverse transcription (RT)-PCR as previously described (19).

Methionine incorporation assay

The AIMP3 MEF cells were incubated with methionine-free DMEM (Gibco) for 30 min, and 1 μCi [^{35}S]methionine (1175 Ci/mmol, PerkinElmer) was added to each well. After the 1 h incubation, the cells were harvested, and the radiolabeled proteins were detected by scintillation counter. For the knockdown of AIMP3 and MRS, HeLa cells were transfected with specific siRNAs and incubated for 72 h before being subjected to the methionine incorporation assay. The experiments were repeated 3 times.

Gel filtration

HeLa cells were transfected with siRNA (si-AIMP3 and si-MRS) and then cultured for 72 h. For size exclusive chromatography, cells were prepared in lysis buffer (50 mM HEPES pH 7.6, 300 mM NaCl, 1 mM EDTA, 10% glycerol, 0.5% Triton X-100 and 1 mM dithiothreitol) containing protease inhibitor cocktail (Calbiochem) and phosphatase inhibitors (10 mM NaF, 12 mM β-glycerophosphate and 1 mM sodiumorthovanadate). After centrifugation, cell lysates were filtered through a 0.22 μm syringe filter. A total of 5 mg protein was loaded onto gel filtration column (Superdex 200 10/300 GL, GE healthcare) in AKTA FPLC system and eluted at the flow rate of 0.4 ml/min with lysis buffer. Proteins of each fraction were separated by SDS-PAGE and analyzed by immunoblotting with specific antibody.

REFERENCES

1. Park, S. G., Ewalt, K. L., and Kim, S. (2005) Functional expansion of aminoacyl-tRNA synthetases and their interacting factors: new perspectives on housekeepers. Trends Biochem. Sci. **30,** 569-574

2. Park, S. G., Choi, E. C., and Kim, S. (2010) Aminoacyl-tRNA synthetase-interacting multifunctional proteins (AIMPs): a triad for cellular homeostasis. IUBMB Life **62,** 296-302

3. Han, J. M., Lee, M. J., Park, S. G., Lee, S. H., Razin, E., Choi, E. C., and Kim, S. (2006) Hierarchical network between the components of the multi-tRNA synthetase complex: implications for complex formation. J. Biol. Chem. **281,** 38663-38667

4. Ko, Y. G., Park, H., Kim, T., Lee, J. W., Park, S. G., Seol, W., Kim, J. E., Lee, W. H., Kim, S. H., Park, J. E., and Kim, S. (2001) A cofactor of tRNA synthetase, p43, is secreted to up-regulate proinflammatory genes. J. Biol. Chem. **276,** 23028-23033

5. Park, S. G., Kang, Y. S., Ahn, Y. H., Lee, S. H., Kim, K. R. Kim, K. W., Koh, G. Y., Ko, Y. G., and Kim, S. (2002) Dose-dependent biphasic activity of tRNA synthetase-associating factor, p43, in angiogenesis. J. Biol. Chem. **277,** 45243-45248

6. Park, S. G., Shin, H., Shin, Y. K., Lee, Y., Choi, E. C., Park, B. J., and Kim, S. (2005) The novel cytokine p43 stimulates dermal fibroblast proliferation and wound repair. Am. J. Pathol. **166,** 387-398

7. Park, S. G., Kang, Y. S., Kim, J. Y., Lee, C. S., Ko, Y. G., Lee, W. J., Lee, K. U., Yeom, Y. I., and Kim, S. (2006) Hormonal activity of AIMP1/p43 for glucose homeostasis. Proc. Natl. Acad. Sci. U.S.A. **103,** 14913-14918

8. Kim, M. J., Park, B. J., Kang, Y. S., Kim, H. J., Park, J. H., Kang, J. W., Lee, S. W., Han, J. M., Lee, H. W., and Kim, S. (2003) Downregulation of FUSE-binding protein and c-myc by tRNA synthetase cofactor p38 is required for lung cell differentiation. Nat. Genet. **34,** 330-336

9. Han, J. M., Park, B. J., Park, S. G., Oh, Y. S., Choi, S. J., Lee, S. W., Hwang, S. K., Chang, S. H., Cho, M. H., and Kim, S. (2008) AIMP2/p38, the scaffold for the multi-tRNA synthetase complex, responds to genotoxic stresses via p53. Proc. Natl. Acad. Sci. U.S.A. **105,** 11206-11211

10. Choi, J. W., Kim, D. G., Park, M. C., Um, J. Y., Han, J. M., Park, S. G., Choi, E. C., and Kim, S. (2009) AIMP2 promotes TNFα-dependent apoptosis via ubiquitin-mediated degradation of TRAF2. J. Cell Sci. **122,** 2710-2715

11. Choi, J. W., Kim, D. G., Lee, A. E., Kim, H. R., Lee, J. Y., Kwon, N. H., Shin, Y. K., Hwang, S. K., Chang, S. H., Cho, M. H., Choi, Y. L., Kim, J., Oh, S. H., Kim, B., Kim, S. Y., Jeon, H. S., Park, J. Y., Kang, H. P., Park, B. J., Han, J. M., and Kim, S. (2011) Cancer-associated splicing variant of tumor suppressor AIMP2/p38: pathological implication in tumorigenesis. PLoS Genet. **7,** e1001351

12. Park, B. J., Kang, J. W., Lee, S. W., Choi, S. J., Shin, Y. K., Ahn, Y. H., Choi, Y. H.,

Choi, D., Lee, K. S., and Kim, S. (2005) The haploinsufficient tumor suppressor p18 upregulates p53 via interactions with ATM/ATR. Cell **120,** 209-221

13. Park, B. J., Oh, Y. S., Park, S. Y., Choi, S. J., Rudolph, C., Schlegelberger, B., and Kim, S. (2006) AIMP3 haploinsufficiency disrupts oncogene-induced p53 activation and genomic stability. Cancer Res. **66,** 6913-6918

14. Oh, Y. S., Kim, D. G., Kim, G., Choi, E. C., Kennedy, B. K., Suh, Y., Park, B. J., and Kim, S. (2010) Downregulation of laminA by tumor suppressor AIMP3/p18 leads to a progeroid phenotype in mice. Aging Cell **9,** 810-822

15. Simos, G., Seqref, A., Fasiolo, F., Hellmuth, K., Shevchenko, A., Mann, M., and Hurt, E. C. (1996) The yeast protein Arc1p binds to tRNA and functions as a cofactor for the methionyl- and glutamyl-tRNA synthetases. EMBO J. **15,** 5437-5448

16. Frechin, M., Kern, D., Martin, R. P., Becker, H. D., and Senger, B. (2010) Arc1p: anchoring, routing, coordinating. FEBS Lett. **584,** 427-433

17. Park, S. G., Jung, K. H., Lee, J. S., Jo, Y. J., Motegi, H., Kim, S., and Shiba, K. (1999) Precursor of pro-apoptotic cytokine modulates aminoacylation activity of tRNA synthetase. J. Biol. Chem. **274,** 16673-16676

18. Quevillon, S., and Mirande, M. (1996) The p18 component of the multisynthetase complex shares a protein motif with the β and γ subunits of eukaryotic elongation factor 1. FEBS Lett. **395,** 63-67

19. Kwon, N. H., Kang, T., Lee, J. Y., Kim, H. H., Kim H. R., Hong, J., Oh, Y. S., Han, J.

M., Ku, M. J., Lee, S. Y., and Kim, S. (2011) Dual role of methionyl-tRNA synthetase in the regulation of translation and tumor suppressor activity of aminoacyl-tRNA synthetase-interacting multifunctional protein-3. Proc. Natl. Acad. Sci. U.S.A. **108,** 19635-19640

20. Sonnenberg, N., and Hinnebusch, A. G. (2009) Regulation of translation initiation in eukaryotes: mechanisms and biological targets. Cell **136,** 731-745

21. Kapp, L. D., and Lorsch, J. R. (2004) GTP-dependent recognition of the methionine moiety on initiator tRNA by translation factor eIF2. J. Mol. Biol. **335,** 923-936

22. Naranda, T., Sirangelo, I., Fabbri, B. J., and Hershey, J. W. (1995) Mutation in the NKXD consensus element indicate that GTP binds to the γ-subunit of translation initiation factor eIF2. FEBS Lett. **372,** 249-252

23. Asano, K., Clayton, J., Shalev, A., and Hinnebusch, A. G. (2000) A multifactor complex of eukaryotic initiation factors, eIF1, eIF2, eIF3, eIF5, and initiator $tRNA^{Met}$ is an important translation initiation intermediate in vivo. Genes Dev. **14**, 2534-2546

24. Shin, B. S., Kim, J. R., Walker, S. E., Dong, J., Lorsch, J. R., and Dever, T. E. (2011) Initiation factor eIF2γ promotes eIF2-GTP-Met-$tRNAi^{Met}$ ternary complex binding to the 40S ribosome. Nat. Struct. Mol. Biol. **18,** 1227-1234

25. Kolitz, S. E., and Lorsch, J. R. (2010) Eukaryotic initiator tRNA: finely tuned and ready for action. FEBS Lett. **584,** 396-404

26. Kang, T. J., Yuzawa, S., and Suga, H. (2008) Expression of histone H3 tails with

combinatorial lysine modifications under the reprogrammed genetic code for the investigation on epigenetic markers. Chem. Biol. **15,** 1166-1174

27. Asano, K., Krishnamoorthy, T., Phan, L., Pavitt, G. D., and Hinnebusch, A. G. (1999) Conserved bipartite motifs in yeast eIF5 and eIF2Bε, GTPase-activating and GDP-GTP exchange factors in translation initiation, mediate binding to their common substrate eIF2. EMBO J. **18,** 6734-1688

28. Farruggio, D., Chaudhuri, J., Maitra, U., and RajBhandary, U. L. (1996) The A1-U72 base pair conserved in eukaryotic initiator tRNAs is important specifically for binding to the eukaryotic translation initiation factor eIF2. Mol Cell Biol. **16,** 4248-4256

CONCLUSION

In this study, I looked at the regulation of translational initiation by MRS and its cofactor AIMP3. In part I, the role of MRS in translational regulation was demonstrated under DNA damage stress, as like UV. Under UV stress, MRS was modified by GCN2 and tumor suppressor activity of AIMP3 was controlled because of this modification. In addition, the catalytic activity of MRS was reduced by blocking of tRNA binding. However, it is still unclear how AIMP3 was dissociated from MSC. Although there is much knowledge regarding ARS modification, there was no report showing whether this modification directly affects the catalytic activity. As a result, the possibility of how protein synthesis can be affected from ARS modification and effect of this modification on the aminoacylation activity was shown to exist. In part II, AIMP3, a cofactor that interacts with MSC, was demonstrated to play a crucial role in protein synthesis. Currently the noncanonical functions of AIMPs are well-known, however the relation of protein synthesis and AIMPs is not identified. In this thesis, AIMP3 delivers charged initiator tRNA to the eIF2 complex, thereby completing the formation of ternary complex.

In conclusion, I have demonstrated the regulation mechanism of translation initiation process by MRS and AIMP3 through the interplay with

each other. MRS and AIMP3 cooperate to control translational initiation for precise and efficient translation. My thesis is significant in that MRS and AIMP3 represent new components for regulator of translational initiation. Through my finding, I expect to reveal new functions of other ARSs and AIMPs in translational regulation.

(국문 초록)

단백질합성 시작 단계에서 Methionyl-tRNA Synthetase 와 AIMP3/p18 의 기능적 의의

강 태 희

약학과 의약생명과학전공

서울대학교 대학원

단백질합성효소 (ARS; aminoacyl-tRNA synthetase)는 고등생물에서 9개의 ARSs와 3개의 보조인자가 multisynthetase complex (MSC)를 이루고 있으며, 그 중에서 methionyl-tRNA synthetase (MRS)는 methionine을 자신의 상보적인 initiator tRNA에 붙여주는 효소로서 암의 억제효과를 가지고 있는 보조인자인 ARS-interacting multifunctional protein 3 (AIMP3)와 결합하고 있다. 위의 두 단백질이 각각 여러 가지 기능을 가지고 있으나 단백질합성과 관련하여 왜 특이적으로 결합을 하고 있는지 그리고 어떻게 조절하는지 아직 밝혀

진 바가 없었다. 본 연구에서는 이 두 단백질이 어떻게 단백질합성에 관여하여 조절하는지 규명하였다. 제 1 단원에서는 단백질합성 및 AIMP3의 암 억제 활성의 조절에 있어서 MRS의 두 가지 역할에 대하여 기술하였다. MRS와 AIMP3는 각각의 GST 유사 부위를 통하여 결합을 하며, 자외선 처리시 그 결합이 떨어지는 것을 확인하였다. 이러한 현상은 general control nonrepressed 2 (GCN2)에 의존적으로 일어나며, GCN2에 의하여 MRS가 662번째 Serine에 인산화되는 것을 볼 수 있었다. 인산화가 된 MRS는 구조변화를 유도하여 AIMP3를 complex에서 놓아주게 되며, 활성 및 전반적인 단백질합성을 줄여주게 됨을 확인할 수 있었다. 또한 자외선과 같은 DNA 손상에 반응하는 eIF2α와 함께 단백질합성 저해를 위해 서로 협력한다는 것을 증명하였다. 이와 같은 기작으로 MRS가 DNA 손상에 관련된 스트레스에 의한 단백질합성 조절 및 암 억제 활성을 조절할 것으로 판단된다. 제 2 단원에서는 AIMP3가 단백질합성 개시 complex로 charged initiator tRNA (Met-tRNAi^{Met})의 전달을 매개함으로써 단백질합성시작 단계를 조절한다는 것을 기술하였다. MRS와의 결합을 통하여 MSC에 속해있는 AIMP3는 MRS에 의해 charge

된 Met-tRNAi^{Met}와 결합한다. 이는 initiator tRNA에 특이적이며, initiator tRNA의 acceptor stem에 결합해 있는 methionine을 인식하여 결합한다. AIMP3와 MRS는 eIF2γ와 각각 결합하며, eIF2α와 γ가 MRS와 AIMP3와 함께 complex를 형성할 수 있음을 확인하였다. 또한 AIMP3는 MRS와 eIF2γ의 결합을 매개하며, 활성화된 eIF2γ가 AIMP3와 결합하는 것을 확인하였다. 마지막으로 AIMP3가 위와 같은 현상을 통하여 3중복합인자 (initiator ternary complex) 형성을 조절하고 이를 통하여 전체적인 단백질합성에 관여함을 밝혔다.

주요어 : MRS, GCN2, eIF2, initiator tRNA, AIMP3, Translation

학번 : 2006-30453